iScience

CellPress

Article

Highly Selective Transmission Success of Dengue Virus Type 1 Lineages in a Dynamic Virus Population: An Evolutionary and Fitness Perspective

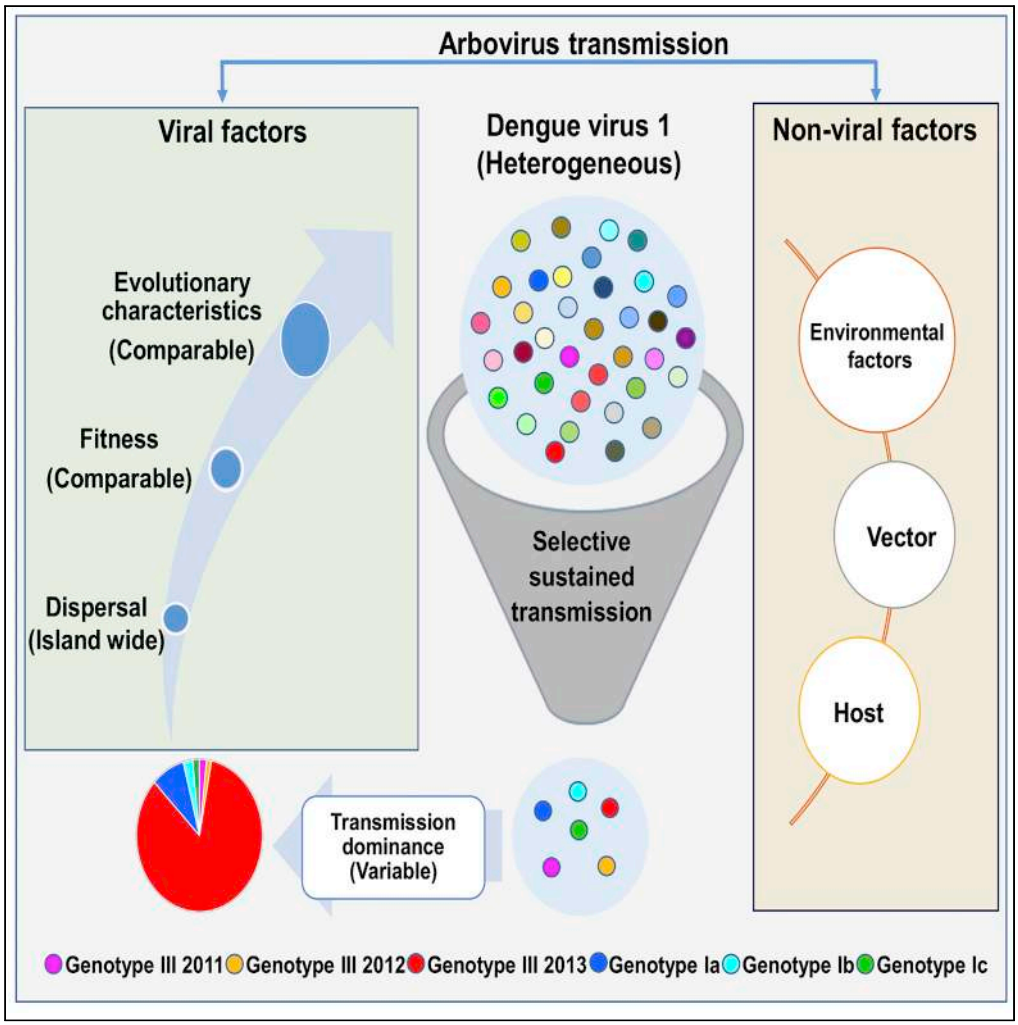

Carmen Koo, Wei Ping Tien, Helen Xu, ..., Yee Ling Lai, Lee-Ching Ng, Hapuarachchige Chanditha Hapuarachchi

chanditha_hapuarachchi@nea.gov.sg

HIGHLIGHTS

The sustained transmission of dengue virus 1 lineages is highly selective

The overall dominance is variable even among the "established" lineages

The lineage dominance is not merely determined by virus evolution and fitness

The non-viral factors play an important role in the survival of virus lineages

Koo et al., iScience 6, 38–51
August 31, 2018
https://doi.org/10.1016/j.isci.2018.07.008

iScience

CellPress

Article

Highly Selective Transmission Success of Dengue Virus Type 1 Lineages in a Dynamic Virus Population: An Evolutionary and Fitness Perspective

Carmen Koo,[1] Wei Ping Tien,[1] Helen Xu,[1] Janet Ong,[1] Jayanthi Rajarethinam,[1] Yee Ling Lai,[1] Lee-Ching Ng,[1,2] and Hapuarachchige Chanditha Hapuarachchi[1,3,*]

SUMMARY

Arbovirus transmission is modulated by host, vector, virus, and environmental factors. Even though viral fitness plays a salient role in host and vector adaptation, the transmission success of individual strains in a heterogeneous population may be stochastic. Our large-scale molecular epidemiological analyses of a dengue virus type 1 population revealed that only a subset of strains (16.7%; n = 6) were able to sustain transmission, despite the population being widely dispersed, dynamic, and heterogeneous. The overall dominance was variable even among the "established" lineages, albeit sharing comparable evolutionary characteristics and replication profiles. These findings indicated that virological parameters alone were unlikely to have a profound effect on the survival of viral lineages, suggesting an important role for non-viral factors in the transmission success of lineages. Our observations, therefore, emphasize the strategic importance of a holistic understanding of vector, human host, and viral factors in the control of vector-borne diseases.

INTRODUCTION

Arthropod-borne viruses (arboviruses) typically survive through horizontal transmission between vertebrate hosts and biting arthropod vectors such as midges, mosquitoes, and ticks. Being RNA viruses, arboviruses demonstrate low fidelity during genome replication (Steinhauer et al., 1992) and exist as diverse populations of closely related variants that collectively behave as "quasispecies" (Domingo et al., 2012). The mutant swarms that constitute "quasispecies" are crucial for virus evolution in dynamic environments. Arboviruses are subjected to evolutionary constraints due to their alternating replication between mammalian and invertebrate hosts (Coffey et al., 2008; Vasilakis et al., 2009). The majority of mutations found in arboviruses, such as Dengue virus (DENV), are deleterious and are eventually weeded out by purifying selection (Holmes, 2003).

DENVs are characterized by extensive genetic diversity and divided into multiple genetically distinct genotypes and lineages (Holmes and Burch, 2000; Holmes and Twiddy, 2003). The genotypes show a characteristic geographical distribution (Holmes and Twiddy, 2003), implying a competitive advantage for individual genotypes in different environments. Rapid evolutionary process of DENV is known to select for strains with enhanced adaptation, generating variants that differ in their ability to spread and cause disease (Twiddy et al., 2002b). The evolutionary dynamics of DENV are influenced by a complex interaction between natural selection and genetic drift, contributing to lineage diversity and dominance (Zhang et al., 2005). The fixation of transient deleterious mutations by stochastic forces is an established phenomenon in DENV populations (Klungthong et al., 2004; Zhang et al., 2005). For instance, seasonal and spatial fluctuations in vector abundance may impose population bottlenecks on endemic strains, thus allowing new viruses to establish in an ecological niche (Scott et al., 2000). In addition, cross-protective immunity among DENV serotypes plays an important role in governing the transmission potential of circulating strains in a particular locality (Adams et al., 2006; Chen and Vasilakis, 2011). The differential susceptibility among new viruses against cross-reactive immune responses elicited by preceding serotypes may give rise to serologic-escape mutants that sustain transmission and cause cyclical epidemics (Adams et al., 2006). These observations suggest that the ability of DENV strains to establish transmission in a given locality is influenced by the epidemiological landscape shaped by a combination of viral, immunological, vector, and environmental determinants (Lourenco and Recker, 2010).

[1]Environmental Health Institute, National Environment Agency, 11, Biopolis Way, #06-05-08, Singapore 138667, Singapore

[2]School of Biological Sciences, Nanyang Technological University, 60 Nanyang Drive, Singapore 637551, Singapore

[3]Lead Contact

*Correspondence: chanditha_hapuarachchi@nea.gov.sg

https://doi.org/10.1016/j.isci.2018.07.008

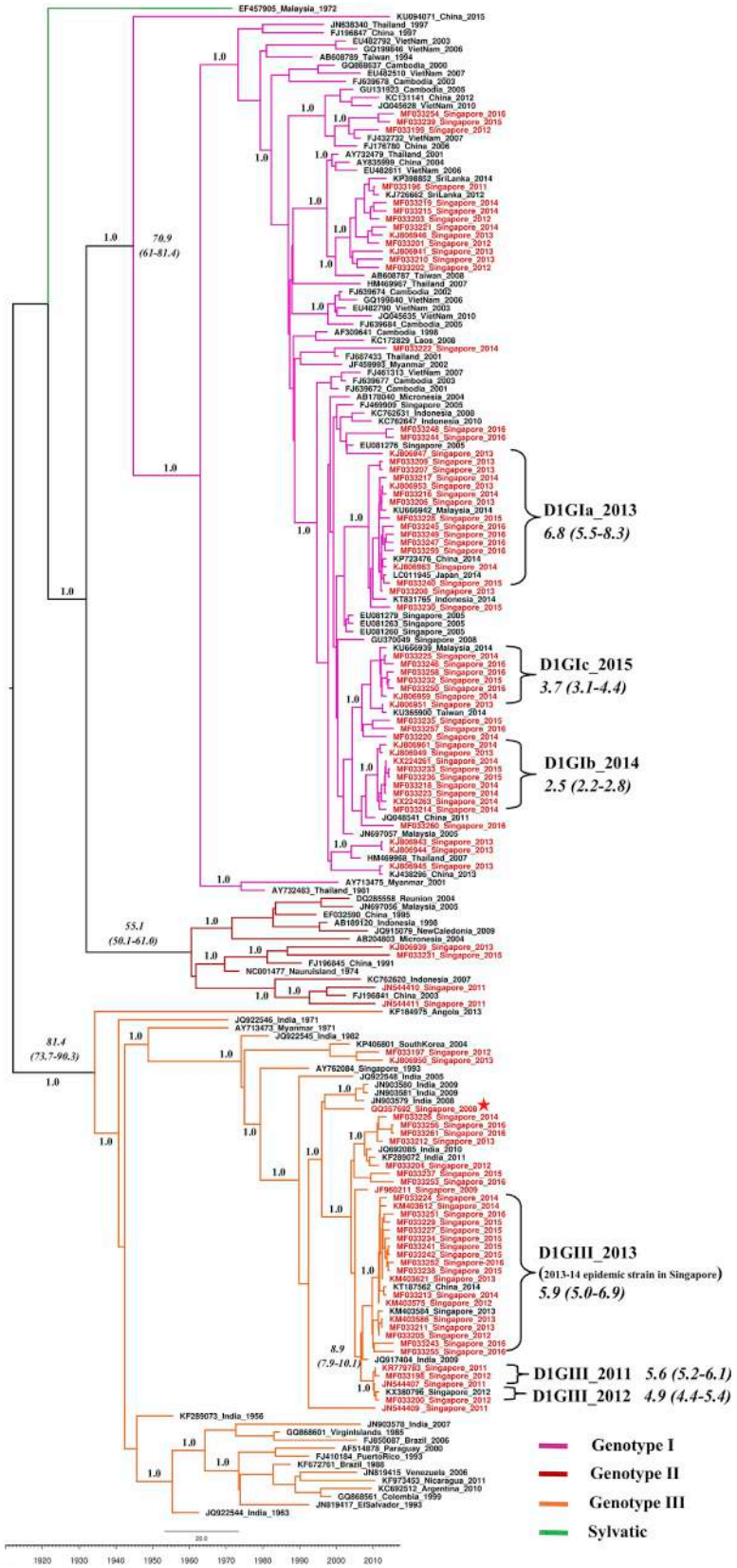
D1GIa_2013
6.8 (5.5-8.3)
D1GIc_2015
3.7 (3.1-4.4)
D1GIb_2014
2.5 (2.2-2.8)
D1GIII_2013
(2013-14 epidemic strain in Singapore)
5.9 (5.0-6.9)
D1GIII_2011 5.6 (5.2-6.1)
D1GIII_2012 4.9 (4.4-5.4)
70.9
(61-81.4)
55.1
(50.1-61.0)
81.4
(73.7-90.3)
8.9
(7.9-10.1)
Genotype I
Genotype II
Genotype III
Sylvatic
1920
1930
1940
1950
1960
1970
1980
1990
2000
2010

Figure 1. Phylogenetic and tMRCA Analysis of DENV-1

The time-scaled maximum clade credibility tree was constructed using the Bayesian Markov Chain Monte Carlo (MCMC) method implemented in the BEAST package v1.7.4. The analysis included 93 complete polyprotein sequences selected to cover all possible viral genetic diversity observed during this study (highlighted in red) and 94 sequences retrieved from GenBank database. Each genotype is shown in different colors as per the tree legend. The local strain (imported case from India) that clustered in the outgroup of genotype III lineages is shown with an asterisk. Numbers on branches represent the posterior probability values. The tMRCA values in years are shown in italics, with 95% highest posterior density (HPD) values in brackets. The scale bar shown above the time scale is substitutions/site/year.

DENV is hyper-endemic in Singapore, where all four serotypes circulate (Lee et al., 2012), with DENV-1 and DENV-2 being the most common. One serotype typically dominates at any given time. The switching of dominant serotypes has been associated with epidemics (Hapuarachchi et al., 2016b; Lee et al., 2010). There have been two large epidemics due to DENV-1 in the country in 2005 (Koh et al., 2008) and 2013–14 (Hapuarachchi et al., 2016a, 2016b). The dominant genotypes during each epidemic were different; genotype I in 2005 (Schreiber et al., 2009) and genotype III in 2013–14 (Hapuarachchi et al., 2016a, 2016b). In addition, the laboratory-based virus surveillance has identified a plethora of less-dominant, yet genetically distinct strains since 2008. Virus surveillance plays an important role in the integrated vector control program in Singapore by providing regular updates on the circulating virus strains, which helps to assess the epidemic risk of any newly emerging virus, and thereby to prioritize control efforts on the ground. Being a vibrant trade and travel hub in a dengue hyper-endemic region, the introduction of new viruses and the rapid evolution of circulating viral lineages sustain the high diversity of DENV in Singapore (Lee et al., 2012). This provides many opportunities to explore the evolutionary processes among DENVs that go through bottlenecks due to dynamic fluctuations of immunological pressure and vector population density.

In the present study, we conducted a molecular epidemiological analysis of DENV-1 genotypes collected island wide between 2011 and 2016, using both envelope (*E*) gene and complete genome sequences. Our aim was to understand the origin, evolution, dispersal, and transmission success of different lineages of DENV-1 circulated during the study period. Considering viral replication in host cells as a surrogate for the fitness, we demonstrate that the variable transmission success of lineages that established sustained transmission is shaped by stochastic forces, which are likely to be influenced by non-viral factors more than the viral fitness and evolutionary differences.

RESULTS AND DISCUSSION

Among 18,696 individuals tested between January 2011 and December 2016, 4,252 patients (22.7%) were positive for DENV NS1 antigen. DENV serotypes were determined in 3,946 (92.8%) NS1-positive sera. DENV-1 (56.7%) was the dominant serotype, followed by DENV-2 (33.5%), DENV-3 (7.6%), DENV-4 (2.1%), and mixed serotypes (0.1%; DENV-1 and DENV-2). Of them, 3,363 samples of all serotypes were genotyped by using *E* gene sequences. The present study reports the analysis of only DENV-1, which includes 1,963 *E* genes and 239 complete polyprotein sequences.

DENV-1 Population was Highly Heterogeneous, but Only Six Lineages Established Sustained Transmission

E gene sequences were used to determine the weekly dynamics of DENV-1 heterogeneity. The *E* gene collection included 29 sequences reported in 2011, 49 in 2012, 728 in 2013, 990 in 2014, 93 in 2015, and 74 in 2016. Whole genome sequencing was performed on a subset of samples selected to represent different groups of viruses identified based on *E* gene phylogeny to understand virus evolution during the study period. In addition, we completed the polyprotein sequences of two genotype III isolates detected in 2008 and 2009 for comparison purposes.

There were 36 genetically distinct DENV-1 strains of multiple lineages (please see the Transparent Methods section for the definition of a strain). Notably, only six (16.7%) of them (genotype III 2011, genotype III 2012, genotype III 2013, genotype Ia, genotype Ib, and genotype Ic) established sustained transmission and formed distinct lineages with strong posterior probability support (Figure 1). Their mean evolutionary rates were comparable (Tables 1 and 2) and consistent with the estimated rates obtained for DENV-1 in previous reports (Sun and Meng, 2013; Twiddy et al., 2003). Each "established" lineage shared a common regional ancestor (Figure 1; Tables 1 and 2), indicating the cross-border virus sharing. The origin and divergence data analyses (Tables 1 and 2) revealed that the emergence period of "established" lineages ranged

DENV-1 Strains	Genome-wide Genetic Signature (Non-synonymous)	Mean Evolutionary Rate[a] (95% HPD)	tMRCA[b] (95% HPD)	Closest Ancestor (Posterior Probability)
GIII 2011	prM-I120M + E-I129T + E-F337I + NS1-D278N	7.3 (2.8–12.7)	5.6 (5.2–6.1)	India 2009 (0.997)
GIII 2012	prM-I120M + E-I129T + E-S449N + NS2A-S142P	8.1 (3.9–14.0)	4.9 (4.4–5.4)	India 2009 (0.997)
GIII 2013	E-F337I + NS1-D278N	5.5 (2.8–8.5)	5.9 (5.0–6.9)	India 2009 (0.976)

Table 1. Summary of Evolutionary Analysis of "Established" Lineages of DENV-1 Genotype III

GIII, genotype III; HPD, highest posterior density; tMRCA, time to most recent common ancestor.

[a]Expressed in $\times 10^{-4}$ nucleotide substitutions/site/year.

[b]Expressed in years, to be calculated from 2016.

from 2008 to 2014 and the median age of each lineage did not differ substantially, suggesting that different virus lineages emerged in a parallel timescale and co-circulated subsequently. Genotype III 2013 was the dominant lineage during the 2013–14 epidemic (Hapuarachchi et al., 2016a, 2016b). Figure 2 shows the time of emergence, extinction, and temporal fluctuations of each "established" lineage from 2011 to 2016.

DENV-1 Strains were Widely Dispersed and Showed Distant Diffusion Pathways

In contrast to other regional countries (Raghwani et al., 2011), our phylogeography analysis revealed a weak spatial clustering of DENV-1 population in Singapore, implying its widespread and complex distribution in local settings (please see the Transparent Methods section for the assigning of location information to sequences). The analysis revealed 35 well-supported (Bayes factor [BF] > 3) diffusion pathways (Figure 3; see Table S1). Of them, 13 pathways demonstrated decisive support (BF > 100). The highest connectivity was observed in clusters 4 (Ang Mo Kio/Serangoon/Hougang), 6 (Kaki Bukit/Ubi/Telok Kurau), 7 (Tampines), and 10 (Yishun/Woodlands), suggesting an important role for these areas in DENV-1 dissemination in the country. The most probable ancestral locations of six "established" strains were in South Central Singapore (Figure 3; see Table S2), which is historically a dengue hot spot. More importantly, among 13 diffusion pathways with BF > 100, 9 (69.2%) were distant links (West-East) (Figure 3). Being a small island, the well-developed transportation network and a highly mobile population could have facilitated the virus spread between distant locations in Singapore. The estimated root state posterior probability was highest in clusters 9 (0.106) and 10 (0.104), followed by clusters 4 (0.103) and 2 (0.103), indicating that they were the major sources of DENV-1 diversity in Singapore (see Figure S1). Clusters 9 and 10 are in close proximity to (approximately 5–10 km) the Woodlands Checkpoint, which is one of the immigration checkpoints, suggesting the potential of virus sharing across the northern border between Singapore and Malaysia (Ng et al., 2015).

DENV-1 Strains	Genome-wide Genetic Signature (Non-synonymous)	Mean Evolutionary Rate[a] (95% HPD)	tMRCA[b] (95% HPD)	Closest Ancestor (Posterior Probability)
GIa	NS1-F323Y + NS2A-M168I + NS5-I114V + NS5-V231I + NS5-N285C + NS5-P525S + NS5-D554E + NS5-L562Q	6.8 (4.6–9.6)	6.8 (5.5–8.3)	Singapore 2005 (0.998)
GIb	preM-V135A + E-S338L + E-T359S + NS2B-L21F + NS4A-V68M + NS5-P137H + NS5-I181V + NS5-V413I + NS5-P525S	8.0 (3.8–13.2)	2.5 (2.2–2.8)	China 2011 (0.998)
GIc	NS2B-I106 + NS5-V413I	7.7 (3.8–12.3)	3.7 (3.1–4.4)	Singapore 2013 (0.998)

Table 2. Summary of Evolutionary Analysis of "Established" Lineages of DENV-1 Genotype I

GI, genotype I; HPD, highest posterior density; tMRCA, time to most recent common ancestor.

[a]Expressed in $\times 10^{-4}$ nucleotide substitutions/site/year.

[b]Expressed in years, to be calculated from 2016.

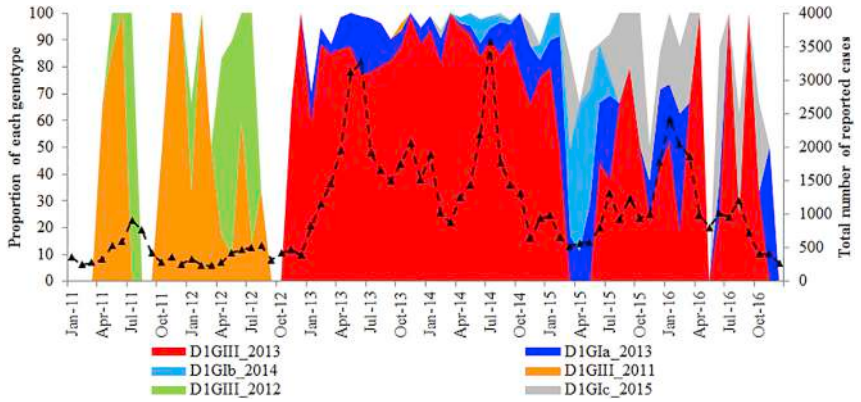

Figure 2. Time of Emergence, Extinction and Temporal Fluctuations of Each "Established" Lineage from 2011 to 2016

The figure was generated based on the genotype information gathered from the analysis of 1,963 complete *E* gene sequences. The longitudinal pattern of total reported cases is shown in a broken line to demonstrate the varying dominance of six "established" lineages during periods of different transmission intensity. D1, DENV-1; GI, genotype I; GIII, genotype III.

"Established" Lineages were Introduced Independently and Evolved Further *In Situ*

Until the emergence of genotype III 2011 in April (E-week 14) 2011 (Figure 2), our surveillance has captured only two DENV-1 genotype III strains reported locally in 2008 and 2009. Whole genomes of both virus strains were included in the current analysis. To decipher the genetic relationship among DENV-1 genotype III lineages reported from 2009 to 2014, we identified a genome-wide 10-amino acid signature that distinguished each lineage (Figure 4). Despite having the highest genetic similarity (99.2%–99.3% of nucleotide and 99.7%–99.8% of amino acid) with the 2009 isolate, genotype III 2011 lineage (n = 9) (prM-I120M,

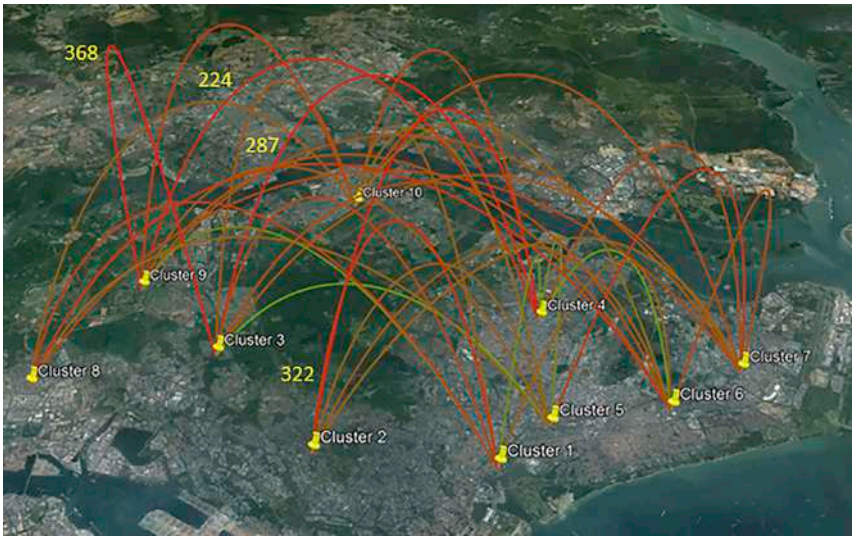

Figure 3. Dispersal Pattern of DENV-1 Population in Singapore from 2011 to 2016

The dataset included 792 complete *E* gene sequences of local DENV-1 isolates, and the sampling locations were classified into 10 clusters; cluster 1, Toa Payoh/Beach Road/Kim Keat Road; cluster 2, Clementi/Leedon Heights; cluster 3, Bukit Batok/Bukit Timah; cluster 4, Ang Mo Kio/Serangoon/Hougang; cluster 5, Geylang; cluster 6, Kaki Bukit/Ubi/Telok Kurau; cluster 7, Tampines; cluster 8, Jurong West/East, cluster 9, Choa Chu Kang/Sungei Kadut; cluster 10, Yishun/Woodlands. The figure shows 35 well-supported epidemiological links (Bayes factor, BF > 3). The branches are colored based on the BF values; red, orange, and green indicate high, intermediate, and low values, respectively. The highest BF values are shown in numbers. See also Figure S1; Tables S1 and S2.

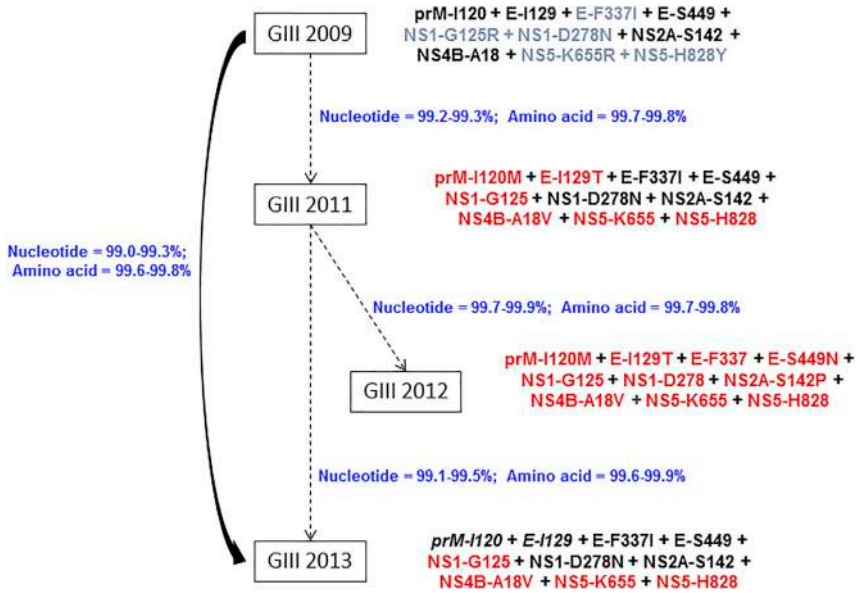

Figure 4. Evolutionary Characteristics of DENV-1 Genotype III Lineages that Established Transmission from 2011 to 2016

The analysis included 144 complete genome sequences of genotype III collected between 2009 and 2016. The isolate in 2009 [SG(EHI)D1/0091Y09] was detected in a sporadic case. It was ancestral to all three "established" genotype III lineages. The 10-amino acid signature is shown next to each lineage/strain, amino acid substitutions in red and reverse mutations in italics. The percentage of nucleotide and amino acid sequence identity is indicated in blue. GIII, genotype III.

E-I129T, and NS4B-A18V) was distinguishable from the 2009 isolate (NS1-G125R, NS5-K655R, and NS5-H828Y) by six amino acid substitutions (Figure 4). Even though the circulation of genotype III lineages was overlapping and successive (Figure 2), mutation patterns showed a unique mixture of forward and reverse substitutions. For an example, prM-I120M and E-I129T substitutions found in genotype III 2011 were wild-type in the genotype III 2013 epidemic lineage. Likewise, E-F337I and NS1-D278N substitutions found in both 2011 and 2013 lineages were wild-type in genotype III 2012 isolates (Figure 4).

This swapping mutation identity lacked a temporal direction and indicated a mixed (forward-reverse) evolutionary pattern. This was further supported by the time to most recent common ancestor (tMRCA) analysis that showed a longer period of emergence (median 5.9 years from 2016; 95% highest posterior density [HPD] 5.0–6.9 years) for the genotype III 2013 epidemic lineage than the 2012 lineage (median 4.9 years from 2016; 95% HPD 4.4–5.4 years). Given the relatively short time gap of emergence between each lineage, limited number of genotype III strains detected during 2009–12, and lack of intermediate sequences, we postulated that DENV-1 genotype III lineages observed since 2011 have been introduced rather than emerging through an *in situ* evolutionary process.

Phylogenetic analysis of whole-genome sequences revealed that DENV-1 sequences reported during 2008–09 from India (GenBank: JN903580, JN903581, and JN903579) formed the outgroup of local genotype III lineages (Figure 1). Another locally reported virus strain (GenBank: GQ357692) that clustered with the "outgroup" sequences (Figure 1) was obtained from an imported case from southern India. Indian sub-continent strains and local genotype III lineages shared a unique genetic signature of C-L46M + NS5-L123I substitutions. Of the two substitutions, NS5-L123I is unique and novel among DENV-1 genotype III sequences known to date. These findings suggested that local genotype III lineages were ancestral to Indian sub-continent isolates. Based on C-prM region sequences from the GenBank database, it was evident that isolates with C-L46M substitution have circulated in northern India in 2010 (GenBank: JF276796) and 2012 (GenBank: KC787088). However, DENV-1 genotype III sequences reported in and before 2006 did not possess the C-L46M substitution (Kukreti et al., 2008; Patil et al., 2011). This observation is in agreement with our tMRCA analysis that suggested the emergence of local genotype III lineages to be between 2006 and 2008 (median 8.9 years from 2016; 95% HPD 7.9–10.1 years).

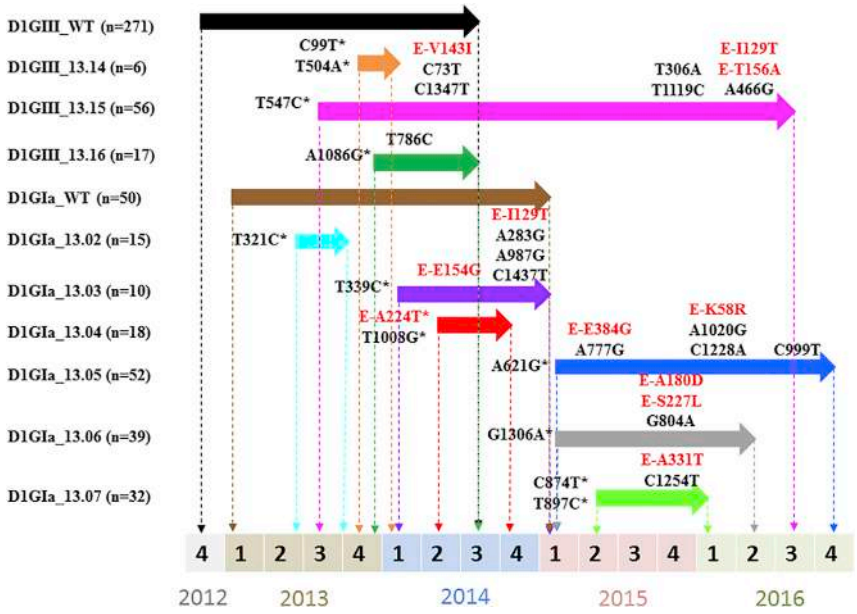

Figure 5. Mutation Profiles of Variants of DENV-1 Genotype III 2013 and Genotype Ia Lineages

The figure illustrates temporal pattern of emergence, maintenance, and extinction of each variant during the study period. The classification of DENV-1 genotype III variants (variant 13.01–13.13) has been described in details elsewhere (Hapuarachchi et al., 2016a). Arrows indicate the transmission period of each variant. A timeline is given below the figure with numbers 1–4 to represent each quarter of the year (1: Jan–Mar; 2: Apr–Jun; 3: Jul–Sep; 4: Oct–Dec). Substitutions shown are the *E*-gene-based signature mutations of each variant. Initial substitutions were considered as founder substitutions and have been shown with an asterisk. Those that appeared later in respective variants were named as "secondary" substitutions (without an asterisk) in the text. Those shown in red are "fixed" non-synonymous substitutions. Remaining residues are "fixed" synonymous substitutions. Positions of all amino acid substitutions are shown at the *E* gene level, whereas the synonymous substitutions are numbered from the beginning of the polyprotein. D1GIII, genotype III 2013 lineage; D1GIa, genotype Ia lineage; n, number of sequences belonging to each variant, WT, wild-type.

Another notable genetic link between the Indian sub-continent strains and local genotype III lineages was a 21-nucleotide deletion (10,296–10,316; GenBank: NC001477) in the hypervariable region (HVR) of the 3′ UTR. The deletion was present in all DENV-1 genotype III sequences that possess C-L46M and NS5-L123I substitutions (see Figure S2). Earlier studies suggest that this 3′ UTR deletion is a unique marker of DENV-1 circulating in the Indian sub-continent from 2006 onward (Dash et al., 2015). Together with our findings, it is evident that a new lineage of DENV-1 genotype III that possessed C-L46M + NS5-L123I substitutions and the 21-nucleotide deletion in 3′ UTR has emerged in the region around 2006.

Among three genotype I lineages (denoted as genotype Ia, Ib, and Ic) that established sustained transmission, genotype Ia was the most common and contributed to the second highest case burden during the 2013–14 epidemic (Hapuarachchi et al., 2016b). Although each genotype I lineage possessed a distinct amino acid signature (Table 2), all three lineages shared several similar features. They were newly emerged viruses circulating in the region at a similar timescale. The tMRCA analysis indicated a recent ancestry for genotypes Ib and Ic (Table 2), approximately at the same time of their emergence in Singapore. All lineages, except genotype Ib, included isolates reported from regional countries during the same period (Figure 1), indicating their widespread presence in Southeast Asia and the possibility of them being introduced into Singapore.

Besides introductions, *in situ* evolution also played an important role in driving the micro-scale diversity of "established" lineages. For example, the detailed analysis of 1,582 complete *E* gene sequences of the genotype III 2013 lineage demonstrated a consistent micro (*in situ*) evolutionary process that is likely to be facilitated by the intense transmission during the epidemic period (Hapuarachchi et al., 2016a). The analysis identified 15 genetically distinguishable variants (wild-type and additional 14 variants) based on

Substitution[a]	Lineage	Selection Pressure Analysis[b]				
		SLAC	FEL	IFEL	FUBAR	MEME
E-I337F	GIII 2011; GIII 2013	Neg (0.01)	Neg (0.004)	Neu	Neg (0.99)	Epi (0.04)
E-S338L	GIb	Neu	Neg (0.04)	Neg (0.05)	Neg (0.93)	Neu
NS1-F323Y	GIa	Neg (0.04)	Neg (0.02)	Neu	Neg (0.99)	Neu
NS2B-L21F	GIb	Neg (0.001)	Neg (<0.001)	Neg (0.04)	Neg (0.99)	Neu
NS2B-I106	GIc	Neg (0.02)	Neg (0.03)	Neu	Neg (0.97)	Neu
NS4A-V68M	GIb	Neg (0.04)	Neg (0.01)	Neu	Neg (0.99)	Neu
NS5-V231I	GIa	Neg (0.04)	Neg (0.01)	Neu	Neg (0.99)	Neu
NS5-N285C	**GIa**	**Neu**	**Pos (0.03)**	**Pos (0.01)**	**Neu**	**Epi (0.002)**

Table 3. Selection Pressure Analysis on Genome-wide Non-synonymous Substitutions Detected in Six "Established" Lineages of DENV-1

[a]NCBI reference genome NC_001477 was used as the wild type sequence.

[b]The data are given for the residues identified in genetic signatures of each "established" lineage (Tables 1 and 2). The table includes only the sites that were either under purifying or positive (shown in bold) by at least three methods. The neutral sites are given in Table S3. p values (SLAC, FEL, IFEL, and MEME) and posterior probability (FUBAR) are given in brackets. E, envelope protein; Epi, episodic selection; GI, genotype I; GIII, genotype III; prM, precursor membrane protein; Neg, purifying selection; Neu, neutral; NS, non-structural proteins; Pos, positive selection.

fixed nucleotide substitutions in *E* gene (Hapuarachchi et al., 2016a). Of them, the evolutionary dynamics of 12 variants have been described in detail elsewhere (Hapuarachchi et al., 2016a). Among the remaining three variants (13.14–13.16), variant 13.16 (n = 17) was the most common group, followed by variants 13.15 (n = 10) and 13.14 (n = 6). Similarly, genotype Ia was also composed of multiple variants. Each variant possessed characteristic founder and non-founder substitutions that distinguished one another (Figure 5).

"Established" Lineages Shared Similar Evolutionary Characteristics, but were Not Equally Dominant

Despite the widespread distribution in the region, there was limited evidence of positive selection in "established" lineages. In general, they were either under purifying selection or evolutionarily neutral in our analysis (Tables 3 and S3). This finding is consistent with the notion that purifying selection generally drives the evolution of DENV (Holmes and Twiddy, 2003; Teoh et al., 2013; Twiddy et al., 2002a, 2002b; Vasilakis and Weaver, 2008). Unlike other RNA viruses, the evolution of arboviruses is constrained by dual replication in mammalian and invertebrate hosts, producing negative fitness trade-offs among traits favored in each host (Deardorff et al., 2011; Novella et al., 1999; Vasilakis et al., 2009). Recent studies have also revealed that DENV intra-host genetic diversity in mosquitoes is largely shaped by genetic drift and purifying selection (Lequime et al., 2016, 2017). The only exception was NS5-N285C substitution uniquely detected in genotype Ia, which was predicted to be under positive selection by fixed effects likelihood (FEL), internal fixed effects likelihood (IFEL), and mixed effect model of evolution (MEME) methods (Table 3). NS5-285 resides within the RNA-dependent RNA polymerase catalytic domain of NS5 (Klema et al., 2016). However, further studies are needed to determine whether NS5-N285C substitution provided any adaptive advantage to genotype Ia. Interestingly, the mean evolutionary rates among "established" lineages were also comparable (Tables 1 and 2). These observations suggested a role for genetic drift in the apparent "selection" of lineages that established sustained transmission.

Even though genotype I lineages demonstrated the ability to establish sustained transmission, the proportions of genotype Ia (8.2%), Ib (2.4%), and Ic (1.7%) were much lower than that of genotype III 2013 epidemic (81.3%) lineage. This was despite the intense transmission conditions that prevailed during the time of their emergence (Figure 2). The sustainability of virus transmission depends on the availability of a susceptible human pool and a vector population. Unlike in humans, flaviviruses cause a long-lived and persistent infection in vector mosquitoes (Salas-Benito and De Nova-Ocampo, 2015). The adult female mosquitoes have a

lifespan of 1–3 weeks depending on the environmental and non-environmental conditions (Christofferson and Mores, 2016; Liu-Helmersson et al., 2014; Maciel-de-Freitas et al., 2007) such as temperature (Goindin et al., 2015; Maciel-de-Freitas et al., 2007), daily temperature fluctuations (Lambrechts et al., 2011), and virus infection (Christofferson and Mores, 2016). As the virus utilizes host cell pathways and resources to replicate, it is unlikely for another similar or closely related virus strain to infect the same mosquito in a subsequent infection, according to the phenomenon of superinfection (homologous) exclusion (Condreay and Brown, 1986). The co-infection, and especially super-infection (Pepin et al., 2008), may result in competition for host resources (Read and Taylor, 2001) and shape the pathogen virulence and transmissibility, thereby affecting its population dynamics (May and Nowak, 1995; Mosquera and Adler, 1998; Nowak and May, 1994). It has previously been shown that C6/36 *Aedes albopictus* cells infected with four DENV serotypes are resistant to heterotypic super-infection (Dittmar et al., 1982). This suggests that when a particular DENV lineage is dominantly transmitted, there is a weak opportunity for lineages introduced subsequently to establish and spread, especially when *Aedes* mosquito population is consistently suppressed. Our observations on genotype I lineages support this notion. For example, genotype Ic was apparent in large clusters in early 2016, although the lineage was first identified in Singapore in February 2014 (Figure 2). Moreover, 57.4% (27/47) of genotype Ib isolates were detected in clustered cases and no other "established" lineages were detected in the majority (76.5%) of those dengue clusters, indicating the highly localized nature of genotype Ib transmission. In Singapore, the *Aedes aegypti* population is controlled through a multi-pronged approach (Hapuarachchi et al., 2016b), and this may explain why lineages other than the epidemic lineage struggled to dominate.

In Vitro Replication Kinetics Suggested that Variable Transmission Success of "Established" Lineages Is Unlikely to Be due to Increased Fitness

To determine whether the improved fitness contributed to the variable transmission success observed among "established" lineages, we compared the *in vitro* replication kinetics of six lineages in mammalian (Huh-7) and mosquito (C6/36) cell lines. We also included two genotype I strains (D1/SG/05K4441DK1/2005 and D1/SG/05K4443DK1/2005) dominant during the epidemic in 2005, the strain [SG(EHI)D1/0091Y09] that was ancestral to all three genotype III lineages (Figure 1), and SG(EHI)D1/09106Y11, an isolate that did not possess the 21-nucleotide deletion in 3′ UTR observed in the genotype III lineages for comparison purposes. SG(EHI)D1/09106Y11 was detected in a sporadic, single case in 2011. All strains showed similar replication profiles in C6/36 *Aedes albopictus* cell line, although the peak titers were variable and strain dependent, but were not significantly different among strains. This observation agrees with previous reports (Tajima et al., 2007), suggesting that vector adaptation is unlikely to explain the variable transmission success of six lineages.

Having seen indifferent replication profiles in mosquito cells, we were first intrigued to investigate whether the 21-nucleotide deletion in the 3′ UTR HVR influenced the replication ability of genotype III lineages in mammalian cells. HVR is located at the first 45 nucleotides of the 3′ UTR of DENV-1. The region accommodates secondary stem-loop structure required for the virus interaction with cellular and viral proteins during the replication process (Dash et al., 2015). Previous studies have proposed that the complete, but not partial, HVR is essential for efficient replication of DENV-1 in mammalian cells (Tajima et al., 2007). A partial deletion of 19 nucleotides (from 15 to 33 nucleotides of HVR) exhibits a negligible effect on the replication of DENV-1 *in vitro* (Tajima et al., 2006). The secondary structure prediction analysis from a recent study demonstrated that the 21-nucleotide deletion does not alter the overall stem-loop structure of the 3′ UTR, suggesting that this partial deletion is unlikely to affect the replication ability of DENV-1. To further confirm this, we compared the replication profiles of genotype III strains with [genotype III 2011, 2012, 2013, and SG(EHI)D1/0091Y09] and without [SG(EHI)D1/09106Y11] the 21-nucleotide deletion in Huh-7 cells. Our analysis showed that the replication patterns were not significantly different between the two groups, suggesting that the deletion does not substantially affect the replication ability of DENV-1 in both mammalian (Figure 6) and mosquito cells (Figure 7).

Then, we compared the replication profiles between genotype I and III strains in mammalian cells. All viruses, except D1/SG/05K4441DK1/2005 and D1/SG/05K4443DK1/2005 of the 2005 epidemic lineage, demonstrated similar replication profiles in Huh-7 cells. They achieved the peak titers at 48 hours post infection (hpi), whereas D1/SG/05K4441DK1/2005 and D1/SG/05K4443DK1/2005 reached the peak titers at 120 hpi. Interestingly, genotype I lineages circulated after 2011 (Ia, Ib, and Ic) and SG(EHI)D1/09106Y11 strain achieved significantly higher peak titers than genotype III strains (t test; p value < 0.0001), albeit their relatively low transmission

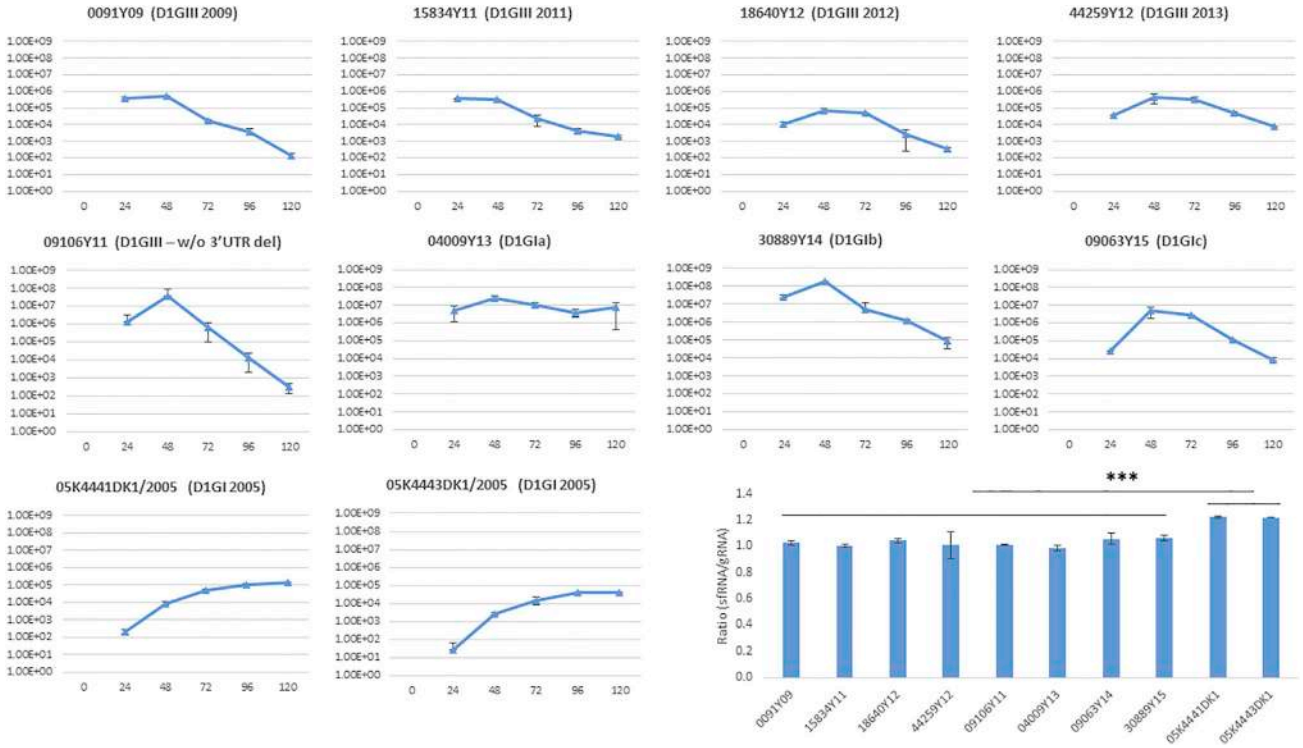

Figure 6. Replication Kinetics and Viral RNA Copy Fluctuations (gRNA and sfRNA) of DENV-1 Lineages and Strains in Huh-7 Mammalian Cells

In vitro experiments were conducted at an MOI of 0.1. The y axis represents virus titers (pfu/mL), whereas the x axis refers to hours post infection (hpi). The bar chart shows the sfRNA:gRNA ratio for each isolate at 24 hpi. SG(EHI)D1/0091Y09, SG(EHI)D1/15834Y11, SG(EHI)D1/18640Y12, and SG(EHI)D1/44259Y12 isolates possess the 21-nucleotide deletion in the hypervariable region of the 3′ UTR (please see also Figure S2). The deletion is absent in SG(EHI)D1/09106Y11; SG(EHI)D1/04009Y13; SG(EHI)D1/30889Y14; SG(EHI)D1/09063Y15; 05K4441DK1/2005; and 05K4443DK1/2005 isolates. D1, DENV-1; GI, genotype I; GIII, genotype III; w/o, without; del, deletion. ***$p \leq 0.001$.

success when compared with genotype III lineages, especially the 2013 epidemic lineage. Moreover, both 2005 genotype I epidemic isolates and genotype Ia sustained virus titers longer than that of the remaining virus strains, in which the titers dropped quickly after 48–72 hpi (Figure 6). Because the number of host cells was comparable at an equal MOI among all virus strains, we postulated that the sustainability of live virus titers in mammalian cells might be explained, at least in part, by the potential ability of respective virus strains to evade the host innate immune response.

It has been proposed previously that excess production of sub-genomic RNA (sfRNA) relative to genomic RNA (gRNA) and sequence variations within the sfRNA region attenuate type I interferon response, and thereby enhance the epidemiological fitness of DENV-2 (Manokaran et al., 2015). Therefore, we investigated the sequence and sfRNA:gRNA copy number variations between genotype I and III strains. The secondary structure prediction based on the full-length DENV-1 3′ UTR revealed that stem loop II (SL II) structures of 2005 genotype I epidemic strains and genotype Ia were similar, but different from other genotype I (Ib and Ic) and genotype III strains (Figure 8). SL II is important for the production of sfRNA (Pijlman et al., 2008), and thus warrants further studies to determine any phenotypic role in observed structural differences. However, the pseudoknot interactions that influence the efficiency of cellular 5′-3′ exoribonuclease and thus modulate the viral ability to generate nuclease-resistant sfRNA (Funk et al., 2010) remained unchanged in all strains (see Figure S3).

Then, we compared the sfRNA:gRNA copy number ratio between genotype I and III strains, obtained by using a newly developed in-house qPCR assay. Interestingly, 2005 genotype I epidemic strains, but not genotype Ia, produced significantly higher sfRNA:gRNA ratios at 24 hpi (Wilcoxon rank-sum test; p value < 0.001). As postulated earlier for DENV-2 (Manokaran et al., 2015), relatively low gRNA produced by 2005 genotype I epidemic strains, especially at early time points, could dampen the interferon response, allowing the virus titers to sustain in mammalian cells (Figure 6). The extended period of live

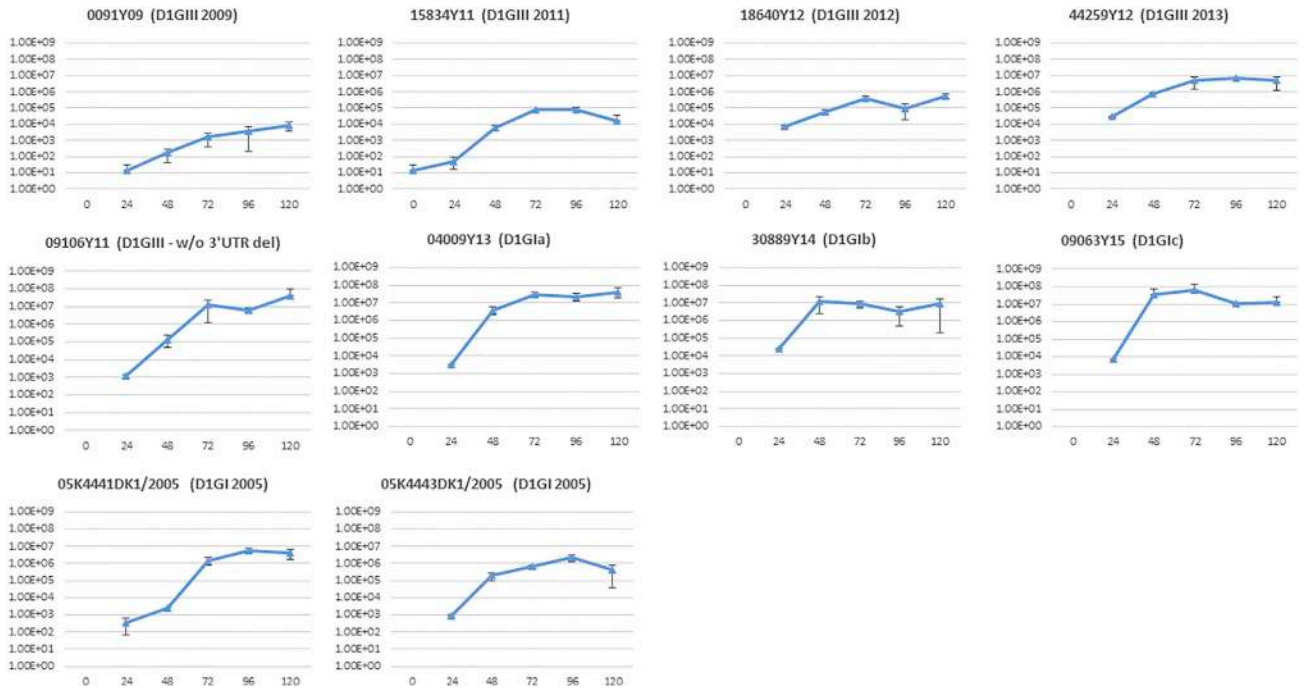

Figure 7. Replication Kinetics and Viral RNA Copy Fluctuations (gRNA and sfRNA) of DENV-1 Lineages and Strains in C6/36 *Aedes albopictus* Cells

In vitro experiments were conducted at an MOI of 0.1. The y-axis represents virus titers (pfu/mL) whereas the x axis refers to hours post infection (hpi). The bar chart shows the sfRNA:gRNA ratio for each isolate at 24 hpi. SG(EHI)D1/0091Y09, SG(EHI)D1/15834Y11, SG(EHI)D1/18640Y12, and SG(EHI)D1/44259Y12 isolates possess the 21-nucleotide deletion in the hypervariable region of the 3′ UTR (please see also Figure S2). The deletion is absent in SG(EHI)D1/09106Y11; SG(EHI)D1/04009Y13; SG(EHI)D1/30889Y14; SG(EHI)D1/09063Y15; 05K4441DK1/2005; and 05K4443DK1/2005 isolates. D1, DENV-1; GI, genotype I; GIII, genotype III; w/o, without; del, deletion.

virus survival could have facilitated transmission and thereby, the epidemic potential. Indeed, both 2005 genotype I strains used in the analysis (D1/SG/05K4441DK1/2005 and D1/SG/05K4443DK1/2005) were epidemic strains (Schreiber et al., 2009). Our findings, therefore, suggest that the "one-two punch" phenomenon (Manokaran et al., 2015) may potentially hold true for other DENV serotypes as well. However, the ratio between sfRNA and gRNA of genotype III strains was not significantly different, despite genotype III 2013 lineage being the dominant strain during the 2013–14 epidemic (Hapuarachchi et al., 2016b), implying that the transmission success and epidemic potential of virus lineages is multifactorial, and may not necessarily be explained by a single phenomenon. Instead, the likely explanation of episodic, epidemic-scale transmission of DENV-1 in Singapore is the reduction of herd immunity against DENV-1 over the decades of DENV-2 predominance. This notion is supported by a recent study that showed low DENV-1 seroprevalance rate (14.2%) among young adults in the country (Low et al., 2015).

In conclusion, although the fitness, evolution, and host adaptation are important determinants of epidemic potential of virus lineages, our findings suggest that non-viral factors also play a substantial role in the transmission success of lineages in heterogeneous virus populations. Notable examples of these non-viral factors are the host immune pressure (herd immunity) and vector abundance. Because we did not perform *in vivo* studies to determine any fitness advantage of "established" strains in local vectors, the probability of vector-virus adaptation cannot be ignored and warrants further studies. Although the monitoring of virus populations is instrumental in identifying the emergence and diffusion of lineages with epidemic potential, our observations emphasize that successful control of vector-borne diseases requires a holistic understanding of vector, human host, and viral factors that contribute to disease transmission.

METHODS

All methods can be found in the accompanying Transparent Methods supplemental file.

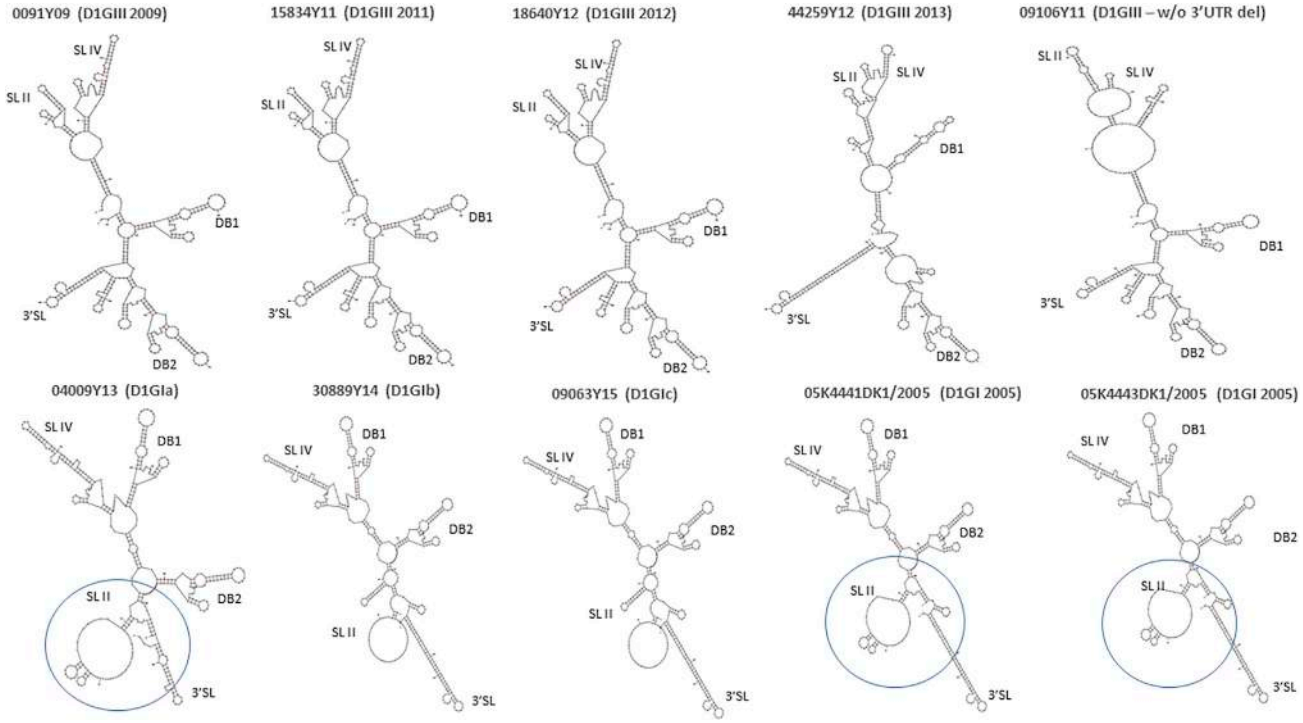

Figure 8. 3′ UTR Structure of DENV-1 Strains

The secondary structure of DENV-1 3′ UTR were predicted using the mfold web server under standard conditions (37°C). The analysis was performed by using complete 3′ UTR sequences. SG(EHI)D1/0091Y09; SG(EHI)D1/15834Y11; SG(EHI)D1/18640Y12; and SG(EHI)D1/44259Y12 isolates possess the 21-nucleotide deletion in the hypervariable region of the 3′ UTR (please see also Figure S2). The deletion is absent in SG(EHI)D1/09106Y11; SG(EHI)D1/04009Y13; SG(EHI)D1/30889Y14; SG(EHI)D1/09063Y15; 05K4441DK1/2005; and 05K4443DK1/2005 isolates. The circles represent SLII structure of 2005 genotype I epidemic strains and genotype Ia. D1, DENV-1; GI, genotype I; GIII, genotype III; SL, stem loop; DB, dumbbell. See also Figure S3.

DATA AND SOFTWARE AVAILABILITY

Sequences used in the phylogenetic analysis, including the representative whole genome sequences, were deposited in Genbank database under the accession numbers GQ357692, JF960211, JN544407, JN544409-JN544411, KJ806939, KJ806941, KJ806943-KJ806947, KJ806949-KJ806951, KJ806953, KJ806959, KJ806961, KJ806963, KR779783, KX224261, KX224263, MF033196-MF033261.

SUPPLEMENTAL INFORMATION

Supplemental Information includes Transparent Methods, three figures, three tables, and two data files and can be found with this article online at https://doi.org/10.1016/j.isci.2018.07.008.

ACKNOWLEDGMENTS

We are grateful to general practitioners in Singapore for providing clinical samples from dengue-suspected patients. We also thank colleagues from the Diagnostics Section at EHI, Singapore, for their support in confirming and serotyping of dengue-positive sera. This study was funded through the core funding from the National Environment Agency, Singapore. The funding sources of this study had no role in the study design, data collection, data analysis, data interpretation, writing of the report, or decision to submit the paper for publication.

AUTHOR CONTRIBUTIONS

H.C.H. conceived the study. Y.L.L. provided patient samples, diagnostic data, and geographic information. C.K., W.P.T. and H.X. performed virus isolation, *in vitro* replication experiments, and genome sequencing. W.P.T. optimized the qPCR assay for the genome copy numbers. H.C.H. and C.K. performed sequence

analyses. J.O. and J.R. performed the geospatial and statistical analyses. H.C.H., C.K., W.P.T., and L.-C.N. wrote the manuscript. All authors reviewed the manuscript.

DECLARATION OF INTERESTS

The authors declare no competing interests.

Received: January 28, 2018
Revised: June 19, 2018
Accepted: July 13, 2018
Published: August 31, 2018

REFERENCES

Adams, B., Holmes, E.C., Zhang, C., Mammen, M.P., Jr., Nimmannitya, S., Kalayanarooj, S., and Boots, M. (2006). Cross-protective immunity can account for the alternating epidemic pattern of dengue virus serotypes circulating in Bangkok. Proc. Natl. Acad. Sci. USA *103*, 14234–14239.

Chen, R., and Vasilakis, N. (2011). Dengue–quo tu et quo vadis? Viruses *3*, 1562–1608.

Christofferson, R.C., and Mores, C.N. (2016). Potential for extrinsic incubation temperature to alter interplay between transmission potential and mortality of dengue-infected *Aedes aegypti*. Environ. Health Insights *10*, 119–123.

Coffey, L.L., Vasilakis, N., Brault, A.C., Powers, A.M., Tripet, F., and Weaver, S.C. (2008). Arbovirus evolution in vivo is constrained by host alternation. Proc. Natl. Acad. Sci. USA *105*, 6970–6975.

Condreay, L.D., and Brown, D.T. (1986). Exclusion of superinfecting homologous virus by Sindbis virus-infected *Aedes albopictus* (mosquito) cells. J. Virol. *58*, 81–86.

Dash, P.K., Sharma, S., Soni, M., Agarwal, A., Sahni, A.K., and Parida, M. (2015). Complete genome sequencing and evolutionary phylogeography analysis of Indian isolates of Dengue virus type 1. Virus Res. *195*, 124–134.

Deardorff, E.R., Fitzpatrick, K.A., Jerzak, G.V., Shi, P.Y., Kramer, L.D., and Ebel, G.D. (2011). West Nile virus experimental evolution in vivo and the trade-off hypothesis. PLoS Pathog. *7*, e1002335.

Dittmar, D., Castro, A., and Haines, H. (1982). Demonstration of interference between dengue virus types in cultured mosquito cells using monoclonal antibody probes. J. Gen. Virol. *59*, 273–282.

Domingo, E., Sheldon, J., and Perales, C. (2012). Viral quasispecies evolution. Microbiol. Mol. Biol. Rev. *76*, 159–216.

Funk, A., Truong, K., Nagasaki, T., Torres, S., Floden, N., Balmori Melian, E., Edmonds, J., Dong, H., Shi, P.Y., and Khromykh, A.A. (2010). RNA structures required for production of subgenomic flavivirus RNA. J. Virol. *84*, 11407–11417.

Goindin, D., Delannay, C., Ramdini, C., Gustave, J., and Fouque, F. (2015). Parity and longevity of *Aedes aegypti* according to temperatures in controlled conditions and consequences on dengue transmission risks. PLoS One *10*, e0135489.

Hapuarachchi, H.C., Koo, C., Kek, R., Xu, H., Lai, Y.L., Liu, L., Kok, S.Y., Shi, Y., Chuen, R.L., Lee, K.S., et al. (2016a). Intra-epidemic evolutionary dynamics of a Dengue virus type 1 population reveal mutant spectra that correlate with disease transmission. Sci. Rep. *6*, 22592.

Hapuarachchi, H.C., Koo, C., Rajarethinam, J., Chong, C.S., Lin, C., Yap, G., Liu, L., Lai, Y.L., Ooi, P.L., Cutter, J., et al. (2016b). Epidemic resurgence of dengue fever in Singapore in 2013-2014: a virological and entomological perspective. BMC Infect. Dis. *16*, 300.

Holmes, E.C. (2003). Patterns of intra- and interhost nonsynonymous variation reveal strong purifying selection in dengue virus. J. Virol. *77*, 11296–11298.

Holmes, E.C., and Burch, S.S. (2000). The causes and consequences of genetic variation in dengue virus. Trends Microbiol. *8*, 74–77.

Holmes, E.C., and Twiddy, S.S. (2003). The origin, emergence and evolutionary genetics of dengue virus. Infect Genet. Evol. *3*, 19–28.

Klema, V.J., Ye, M., Hindupur, A., Teramoto, T., Gottipati, K., Padmanabhan, R., and Choi, K.H. (2016). Dengue virus nonstructural protein 5 (NS5) assembles into a dimer with a unique methyltransferase and polymerase interface. PLoS Pathog. *12*, e1005451.

Klungthong, C., Zhang, C., Mammen, M.P., Jr., Ubol, S., and Holmes, E.C. (2004). The molecular epidemiology of dengue virus serotype 4 in Bangkok, Thailand. Virology *329*, 168–179.

Koh, B.K., Ng, L.C., Kita, Y., Tang, C.S., Ang, L.W., Wong, K.Y., James, L., and Goh, K.T. (2008). The 2005 dengue epidemic in Singapore: epidemiology, prevention and control. Ann. Acad. Med. Singapore *37*, 538–545.

Kukreti, H., Chaudhary, A., Rautela, R.S., Anand, R., Mittal, V., Chhabra, M., Bhattacharya, D., Lal, S., and Rai, A. (2008). Emergence of an independent lineage of dengue virus type 1 (DENV-1) and its co-circulation with predominant DENV-3 during the 2006 dengue fever outbreak in Delhi. Int. J. Infect. Dis. *12*, 542–549.

Lambrechts, L., Paaijmans, K.P., Fansiri, T., Carrington, L.B., Kramer, L.D., Thomas, M.B., and Scott, T.W. (2011). Impact of daily temperature fluctuations on dengue virus transmission by *Aedes aegypti*. Proc. Natl. Acad. Sci. USA *108*, 7460–7465.

Lee, K.S., Lai, Y.L., Lo, S., Barkham, T., Aw, P., Ooi, P.L., Tai, J.C., Hibberd, M., Johansson, P., Khoo, S.P., et al. (2010). Dengue virus surveillance for early warning, Singapore. Emerg. Infect. Dis. *16*, 847–849.

Lee, K.S., Lo, S., Tan, S.S., Chua, R., Tan, L.K., Xu, H., and Ng, L.C. (2012). Dengue virus surveillance in Singapore reveals high viral diversity through multiple introductions and in situ evolution. Infect. Genet. Evol. *12*, 77–85.

Lequime, S., Fontaine, A., Ar Gouilh, M., Moltini-Conclois, I., and Lambrechts, L. (2016). Genetic drift, purifying selection and vector genotype shape dengue virus intra-host genetic diversity in mosquitoes. PLoS Genet. *12*, e1006111.

Lequime, S., Richard, V., Cao-Lormeau, V.M., and Lambrechts, L. (2017). Full-genome dengue virus sequencing in mosquito saliva shows lack of convergent positive selection during transmission by *Aedes aegypti*. Virus Evol. *3*, vex031.

Liu-Helmersson, J., Stenlund, H., Wilder-Smith, A., and Rocklov, J. (2014). Vectorial capacity of *Aedes aegypti*: effects of temperature and implications for global dengue epidemic potential. PLoS One *9*, e89783.

Lourenco, J., and Recker, M. (2010). Viral and epidemiological determinants of the invasion dynamics of novel dengue genotypes. PLoS Negl. Trop. Dis. *4*, e894.

Low, S.L., Lam, S., Wong, W.Y., Teo, D., Ng, L.C., and Tan, L.K. (2015). Dengue Seroprevalence of healthy adults in Singapore: serosurvey among blood donors, 2009. Am. J. Trop. Med. Hyg. *93*, 40–45.

Maciel-de-Freitas, R., Codeco, C.T., and Lourenco-de-Oliveira, R. (2007). Daily survival rates and dispersal of *Aedes aegypti* females in Rio de Janeiro, Brazil. Am. J. Trop. Med. Hyg. *76*, 659–665.

Manokaran, G., Finol, E., Wang, C., Gunaratne, J., Bahl, J., Ong, E.Z., Tan, H.C., Sessions, O.M., Ward, A.M., Gubler, D.J., et al. (2015). Dengue subgenomic RNA binds TRIM25 to inhibit interferon expression for epidemiological fitness. Science *350*, 217–221.

May, R.M., and Nowak, M.A. (1995). Coinfection and the evolution of parasite virulence. Proc. Biol. Sci. *261*, 209–215.

Mosquera, J., and Adler, F.R. (1998). Evolution of virulence: a unified framework for coinfection and superinfection. J. Theor. Biol. *195*, 293–313.

Ng, L.C., Chem, Y.K., Koo, C., Mudin, R.N., Amin, F.M., Lee, K.S., and Kheong, C.C. (2015). 2013 Dengue outbreaks in Singapore and Malaysia caused by different viral strains. Am. J. Trop. Med. Hyg. *92*, 1150–1155.

Novella, I.S., Hershey, C.L., Escarmis, C., Domingo, E., and Holland, J.J. (1999). Lack of evolutionary stasis during alternating replication of an arbovirus in insect and mammalian cells. J. Mol. Biol. *287*, 459–465.

Nowak, M.A., and May, R.M. (1994). Superinfection and the evolution of parasite virulence. Proc. Biol. Sci. *255*, 81–89.

Patil, J.A., Cherian, S., Walimbe, A.M., Patil, B.R., Sathe, P.S., Shah, P.S., and Cecilia, D. (2011). Evolutionary dynamics of the American African genotype of dengue type 1 virus in India (1962-2005). Infect. Genet. Evol. *11*, 1443–1448.

Pepin, K.M., Lambeth, K., and Hanley, K.A. (2008). Asymmetric competitive suppression between strains of dengue virus. BMC Microbiol. *8*, 28.

Pijlman, G.P., Funk, A., Kondratieva, N., Leung, J., Torres, S., van der Aa, L., Liu, W.J., Palmenberg, A.C., Shi, P.Y., Hall, R.A., et al. (2008). A highly structured, nuclease-resistant, noncoding RNA produced by flaviviruses is required for pathogenicity. Cell Host Microbe *4*, 579–591.

Raghwani, J., Rambaut, A., Holmes, E.C., Hang, V.T., Hien, T.T., Farrar, J., Wills, B., Lennon, N.J., Birren, B.W., Henn, M.R., et al. (2011). Endemic dengue associated with the co-circulation of multiple viral lineages and localized density-dependent transmission. PLoS Pathog. *7*, e1002064.

Read, A.F., and Taylor, L.H. (2001). The ecology of genetically diverse infections. Science *292*, 1099–1102.

Salas-Benito, J.S., and De Nova-Ocampo, M. (2015). Viral Interference and persistence in mosquito-borne flaviviruses. J. Immunol. Res. *2015*, 873404.

Schreiber, M.J., Holmes, E.C., Ong, S.H., Soh, H.S., Liu, W., Tanner, L., Aw, P.P., Tan, H.C., Ng, L.C., Leo, Y.S., et al. (2009). Genomic epidemiology of a dengue virus epidemic in urban Singapore. J. Virol. *83*, 4163–4173.

Scott, T.W., Morrison, A.C., Lorenz, L.H., Clark, G.G., Strickman, D., Kittayapong, P., Zhou, H., and Edman, J.D. (2000). Longitudinal studies of *Aedes aegypti* (Diptera: Culicidae) in Thailand and Puerto Rico: population dynamics. J. Med. Entomol. *37*, 77–88.

Steinhauer, D.A., Domingo, E., and Holland, J.J. (1992). Lack of evidence for proofreading mechanisms associated with an RNA virus polymerase. Gene *122*, 281–288.

Sun, Y., and Meng, S. (2013). Evolutionary history and spatiotemporal dynamics of dengue virus type 1 in Asia. Infect. Genet. Evol. *16*, 19–26.

Tajima, S., Nukui, Y., Ito, M., Takasaki, T., and Kurane, I. (2006). Nineteen nucleotides in the variable region of 3′ non-translated region are dispensable for the replication of dengue type 1 virus in vitro. Virus Res. *116*, 38–44.

Tajima, S., Nukui, Y., Takasaki, T., and Kurane, I. (2007). Characterization of the variable region in the 3′ non-translated region of dengue type 1 virus. J. Gen. Virol. *88*, 2214–2222.

Teoh, B.T., Sam, S.S., Tan, K.K., Johari, J., Shu, M.H., Danlami, M.B., Abd-Jamil, J., MatRahim, N., Mahadi, N.M., and AbuBakar, S. (2013). Dengue virus type 1 clade replacement in recurring homotypic outbreaks. BMC Evol. Biol. *13*, 213.

Twiddy, S.S., Farrar, J.J., Vinh Chau, N., Wills, B., Gould, E.A., Gritsun, T., Lloyd, G., and Holmes, E.C. (2002a). Phylogenetic relationships and differential selection pressures among genotypes of dengue-2 virus. Virology *298*, 63–72.

Twiddy, S.S., Holmes, E.C., and Rambaut, A. (2003). Inferring the rate and time-scale of dengue virus evolution. Mol. Biol. Evol. *20*, 122–129.

Twiddy, S.S., Woelk, C.H., and Holmes, E.C. (2002b). Phylogenetic evidence for adaptive evolution of dengue viruses in nature. J. Gen. Virol. *83*, 1679–1689.

Vasilakis, N., Deardorff, E.R., Kenney, J.L., Rossi, S.L., Hanley, K.A., and Weaver, S.C. (2009). Mosquitoes put the brake on arbovirus evolution: experimental evolution reveals slower mutation accumulation in mosquito than vertebrate cells. PLoS Pathog. *5*, e1000467.

Vasilakis, N., and Weaver, S.C. (2008). The history and evolution of human dengue emergence. Adv. Virus Res. *72*, 1–76.

Zhang, C., Mammen, M.P., Jr., Chinnawirotpisan, P., Klungthong, C., Rodpradit, P., Monkongdee, P., Nimmannitya, S., Kalayanarooj, S., and Holmes, E.C. (2005). Clade replacements in dengue virus serotypes 1 and 3 are associated with changing serotype prevalence. J. Virol. *79*, 15123–15130.

ISCI, Volume *6*

Supplemental Information

Highly Selective Transmission Success of Dengue Virus Type 1 Lineages in a Dynamic Virus Population: An Evolutionary and Fitness Perspective

Carmen Koo, Wei Ping Tien, Helen Xu, Janet Ong, Jayanthi Rajarethinam, Yee Ling Lai, Lee-Ching Ng, and Hapuarachchige Chanditha Hapuarachchi

Supplemental figures

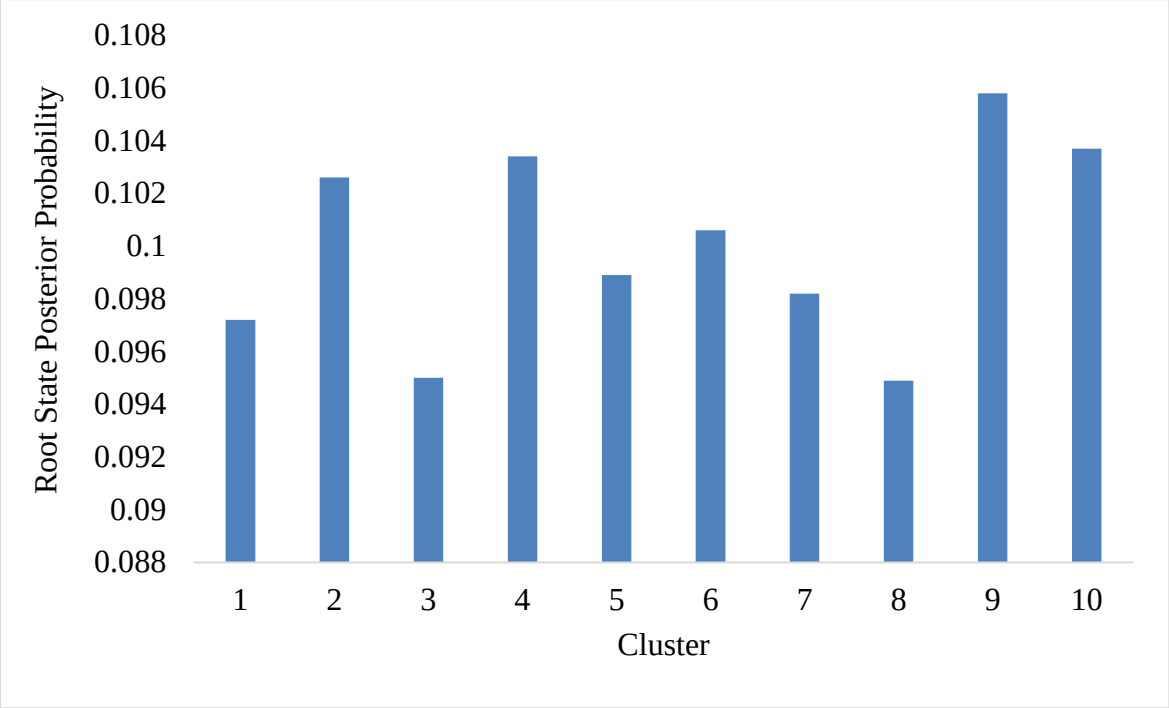

Figure S1. Related to Figure 3. Root state posterior probability of DENV-1.

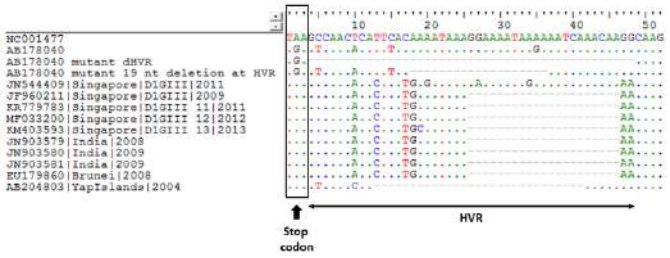

Figure S2. Related to Figures 6, 7 and 8. Schematic diagram of nucleotide deletions reported in the hypervariable region (HVR) of 3'UTR of DENV-1. Dashed lines represent nucleotide deletions. The figure includes global reference strains retrieved from Genbank database (NC001477, AB178040, JN903579, JN903580, JN903581, EU179860 and AB204803) for comparison. D1GIII: DENV-1 genotype III; D1GIII_11: DENV-1 genotype III 2011; D1GIII_12: DENV-1 genotype III 2012; D1GIII_13: DENV-1 genotype III 2013.

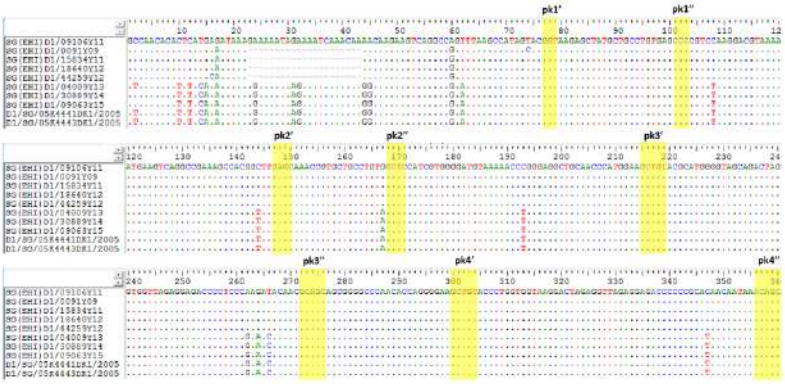

Figure S3. Related to Figure 8. Schematic diagram of putative pseudoknot-forming residues in 3'UTR of DENV-1. The diagram represents positions 1-360 after the stop codon. Regions highlighted in yellow refer to the predicted pseudoknot-forming sequences where base-pairing can occur to form the pseudoknot (pk) structures.

Supplemental tables

Table S1. Related to Figure 3. Bayes factor values of diffusion pathways.

No.	Clusters	Bayes factor value
1	between Cluster 3 and Cluster 9	368.4816194
2	between Cluster 2 and Cluster 4	322.0686685
3	between Cluster 3 and Cluster 4	286.9818883
4	between Cluster 4 and Cluster 9	224.2577204
5	between Cluster 1 and Cluster 2	186.974222
6	between Cluster 6 and Cluster 8	171.1916487
7	between Cluster 5 and Cluster 7	154.3323991
8	between Cluster 9 and Cluster 10	152.2193439
9	between Cluster 1 and Cluster 8	137.3399383
10	between Cluster 4 and Cluster 10	115.5293902
11	between Cluster 7 and Cluster 8	108.8632512
12	between Cluster 1 and Cluster 3	106.9446763
13	between Cluster 7 and Cluster 10	101.2540419
14	between Cluster 6 and Cluster 7	93.93485338
15	between Cluster 4 and Cluster 7	93.69136385
16	between Cluster 3 and Cluster 6	91.14921522
17	between Cluster 7 and Cluster 9	81.51131661
18	between Cluster 3 and Cluster 10	78.51693016
19	between Cluster 3 and Cluster 7	74.8352818
20	between Cluster 6 and Cluster 9	74.71606689
21	between Cluster 2 and Cluster 6	70.73170263
22	between Cluster 5 and Cluster 9	66.26096191
23	between Cluster 8 and Cluster 10	63.24082002
24	between Cluster 1 and Cluster 10	59.92942675

25	between Cluster 1 and Cluster 6	58.75353967
26	between Cluster 2 and Cluster 5	58.6198634
27	between Cluster 2 and Cluster 7	53.4630253
28	between Cluster 5 and Cluster 8	50.5958405
29	between Cluster 6 and Cluster 10	47.00862332
30	between Cluster 5 and Cluster 10	46.06235802
31	between Cluster 4 and Cluster 5	24.04903629
32	between Cluster 1 and Cluster 9	23.84063346
33	between Cluster 1 and Cluster 4	19.53090586
34	between Cluster 4 and Cluster 6	14.80692466
35	between Cluster 3 and Cluster 5	12.90426014

Table shows only the diffusion links with Bayes factor values greater than 3.

Table S2. Related to Figure 3. Summary of the most probable location of origin for each established strain of DENV-1.

DENV-1 strains	Most probable local origin	Root State Posterior Probability	Location of first reported sequence
Genotype III 2011	Cluster 4	0.2097	Cluster 1
Genotype III 2012	**Cluster 6**	**0.544**	**Cluster 6**
Genotype III 2013	Cluster 6	0.1766	Cluster 4
Genotype Ia 2013	Cluster 6	0.1445	Cluster 9
Genotype Ib 2014	**Cluster 4**	**0.2745**	**Cluster 4**
Genotype Ic 2015	**Cluster 4**	**0.6459**	**Cluster 4**

DENV-1 strains, of which the most probable root state matches to the location of its first detected sequence, are shown in bold.

Table S3. Related to Table 3. Neutral sites among the non-synonymous substitutions detected in six "established" lineages of DENV-1

Substitution[¶]	Lineage	Selection Pressure analysis[£]				
		SLAC	FEL	IFEL	FUBAR	MEME
prM-I120M	GIII 2011; DIII 2012	Neu	Neu	Neu	Neg (0.99)	Neu
prM-V135A	GIb	Neu	Neu	Neu	Neg (0.99)	Neu
E-I129T	GIII 2011; GIII 2012	Neu	Neu	Neu	Neg (0.93)	Neu
E-T359S	GIb	Neu	Neu	Neu	Neu	Epi (0.04)
E-S449N	GIII 2012	Neu	Neu	Neu	Neg (0.98)	Neu
NS1-D278N	GIII 2011; GIII 2013	Neu	Neu	Neu	Neu	Neu
NS2A-S142P	GIII 2012	Neu	Neu	Neu	Neu	Neu
NS2A-M168I	GIa	Neu	Neu	Neu	Neu	Neu
NS5-I114V	GIa	Neu	Neu	Neu	Neg (0.94)	Neu
NS5-P137H	GIb	Neu	Neu	Neu	Neg (0.98)	Neu
NS5-I181V	GIb	Neu	Neu	Neu	Neu	Neu
NS5-V413I	GIb; GIc	Neu	Neu	Neu	Neu	Neu
NS5-P525S	GIa; GIb	Neu	Neg (0.03)	Neu	Neg (0.98)	Neu

NS5-D554E	GIa	Neu	Neu	Neu	Neu	Neu
NS5-L562Q	GIa	Neu	Neu	Neu	Neg (0.95)	Neu

[¶]NCBI reference genome NC_001477 was used as the wild type sequence
[£]The data is given for the residues identified in genetic signatures of each "established" lineage (Tables 1 and 2). The table includes only the neutral sites determined by at least three methods. The sites under purifying and positive selection are given in Table 3. P-values (SLAC, FEL, IFEL and MEME) and posterior probability (FUBAR) are given in brackets. E=envelope protein; Epi=episodic selection; GI=genotype I; GIII=genotype III; prM=Precursor membrane protein; Neg=purifying selection; Neu=neutral; NS=non-structural proteins; Pos=positive selection

Transparent Methods

Sample collection

Whole blood samples of dengue-suspected patients were received by the Environmental Health Institute (EHI) from an extensive network of hospitals and general practitioner clinics located throughout Singapore. The present study included samples received by EHI from 2011 to 2016.

Ethics statement

All DENV-positive sera used for the genome sequencing were collected after obtaining the written informed consent from respective patients. All sera were utilized in accordance with the guidelines approved by the Institutional Review Board of National Environmental Agency, Singapore (IRB003.1).

Diagnosis of Dengue virus infections

In Singapore, the detection of NS1 antigen is used as the primary criterion for the confirmation of acute dengue infections. In the present study, Dengue virus (DENV) infection was confirmed by using the SD Bioline Dengue Duo kit (Standard Diagnostics INC., South Korea). SD Bioline Dengue Duo kit is a one-step rapid diagnostic test designed to detect both NS1 antigen and antibodies to DENV (Dengue IgG/IgM) in human serum, plasma or whole blood. The kit has demonstrated 93.9% sensitivity and 92.0% specificity in local cohorts (Gan et al., 2014).

Serotyping of DENV

The serotype of DENV in each NS1 positive sample was determined by using a protocol described elsewhere (Lai et al., 2007). DENV RNA was extracted from 140 µl of each sample serum by using the QIAamp Viral RNA Mini Kit (QIAGEN, Hilden, Germany), according to the manufacturer's guidelines. Forty units of RNaseOUT, a ribonuclease inhibitor (Life Technologies Corporation, USA), were added to each RNA elute to minimize degradation. Real-time reverse transcription polymerase chain reaction (rRT-PCR) was carried out in LightCycler 2.0 (Roche Diagnostics GmbH, Mannheim, Germany), by using the LightCycler RNA Master Hyb Probe Kit (Roche Diagnostics GmbH, Mannheim, Germany). The10 µl reaction mixture included 1X LightCycler RNA Master Hyb Probe mix, 3.25 mM of $Mn(Oac)_2$, 0.3 µM of each primer, 0.3 µM of DENV-1 probe, 0.15 µM of DENV-2 probe, 0.12 µM of DENV-3 probe and 0.2 µM of DENV-4 probe. The primer and probe sequences are available elsewhere (Lai et al., 2007). All reactions included 1 µl of RNA template, except for the negative controls, in which

RNA was replaced with molecular grade water. The single cycle reverse transcription step was carried out at 61^0C for 20 min, followed by 95^0C for 1 min. The amplification cycle included 45 cycles of denaturation at 95^0C for 1 sec, annealing at 59^0C for 15 sec and extension at 72^0C for 10 sec. The melting curves were acquired through a single cycle of 95^0C for 30 sec, followed by a continuous acquisition mode from 95^0C to 40^0C at a slope of 0.1^0C per sec. The melting curves and amplification curves were obtained by using the LightCycler Data Analysis Software version 4.05 (Roche Diagnostics GmbH, Mannheim, Germany).

Isolation of DENV for genome sequencing

DENV was isolated from sera using the *Ae. albopictus* C6/36 mosquito cell line (ATCC CRL-1660). Briefly, the monolayer of C6/36 cells at ~80% confluence was inoculated with 50 µl of serum in L-15 maintenance medium containing 3 % FCS at 33°C to allow for virus adsorption and replication. The infected fluid was harvested after 5-10 days. The presence of DENV in cell supernatants was confirmed by an immunofluoresent assay (IFA), during which cells were reacted with either DENV group-specific or serotype-specific monoclonal antibodies derived from hybridoma cultures (ATCC HB-46, HB-47, HB-48, and HB-49). The fluorescein isothiocyanate-conjugated goat anti-mouse antibody was used as the detector. Based on the original virus load, a maximum of three passages was done for each sample to minimize the cell-culture adaptive mutations.

Sequencing of envelope gene and whole genome of DENV

Envelope *(E)* gene sequences were generated directly from patient sera and the whole genomes were generated from isolates obtained from selected patient sera. Samples for whole genome sequencing were selected to represent different groups of viruses identified based on *E* gene phylogeny to cover observed genetic diversity of local DENV-1 population. For each virus group, genomes of at least two isolates detected throughout their transmission period, particularly during the early and late phases of their presence in the same locality, were fully sequenced. The number of isolates selected from each group was based on the total number of *E* gene sequences available for respective groups.

Complementary DNA (cDNA) was synthesised from extracted RNA by using ProtoScript II First Strand cDNA Synthesis system (New England Biolabs, Massachusetts, USA) according to the recommended protocol. The complete *E* gene (~1.5 kb) and complete genome were amplified by PCR using 0.5 µM of DENV serotype-specific primers and 1X PhusionTM Flash High-Fidelity PCR Master Mix (Finnzymes, Lafayette, CO). The amplification protocol for both *E* gene and the complete genome was as follows: initial denaturation at 98°C for 5 sec, 35 cycles of denaturation at 98°C for 5 sec, annealing at 60°C for 8 sec, extension at 72°C for 25 sec and final extension at 72°C for 1 min. The primers used for the amplifications have previously been described (Koo et al., 2013). Amplified products were purified using GeneJET PCR purification kit (Thermo Scientific, Massachusetts, USA) according to manufacturer's instructions. Sequencing of purified PCR products was performed at a commercial facility according to the BigDye Terminator Cycle Sequencing kit (Applied Biosystems, USA) protocol.

Assembly and analysis of genome sequences

Raw nucleotide sequences were assembled using the Lasergene package version 8.0 (DNASTAR Inc., Madison, WI, USA). Contiguous sequences were aligned using BioEdit 7.0.5 software

suite(Hall, 1999). Whole genome (n=239) and *E* gene (n=792) sequences analysed in the present study were compared with whole genome sequences (n=1768) retrieved from the GenBank database in BioEdit 7.0.5 software suite (Hall, 1999) to identify unique substitutions and genetic signatures of study isolates.

Data and software availability

Sequences used in the phylogenetic analysis, including the representative whole genome sequences, were deposited in Genbank database under the accession numbers GQ357692, JF960211, JN544407, JN544409-JN544411, KJ806939, KJ806941, KJ806943-KJ806947, KJ806949-KJ806951, KJ806953, KJ806959, KJ806961, KJ806963, KR779783, KX224261, KX224263, MF033196-MF033261.

Definition of a strain

DENV is composed of four serotypes and each serotype includes multiple genotypes. Each genotype is a broad classification to allow genetically diverse strains from different geographical regions to be clustered together. The empirical evidence shows that the envelope gene nucleotide divergence cut-off for DENV-1 strains of different genotypes ranges from 1.6% to 5.6% (Goncalvez et al., 2002). In a recent study, we demonstrated that DENV-1 epidemic strains are composed of multiple variants that show less than 1% nucleotide divergence (Hapuarachchi et al., 2016). Therefore, a strain was defined based on >= 1% nucleotide divergence and at least 80% bootstrap support in the *E* gene phylogeny. Besides the % nucleotide distance, 80% bootstrap support was considered to provide phylogenetic robustness of any defined strain.

Phylogenetic analysis of complete polyprotein sequences

A maximum clade credibility (MCC) tree was constructed using Markov Chain Monte Carlo (MCMC) method available in the Bayesian Evolutionary Analysis by Sampling Trees (BEAST) software package v1.7.4 (Drummond and Rambaut, 2007). The dataset included the representative DENV-1 whole polyprotein sequences of 93 study isolates and 94 sequences retrieved from the GenBank database. Out of 239 whole genome sequences, a subset of sequences (n=93) was selected to represent each group of viruses included in the whole genome sequencing. This subset included sequences reported during different time periods to capture the temporal variations, regardless of the locality, because the geography was not a consideration of the phylogenetic analysis. This “subset” selection was done to minimize the overcrowding of phylogeny.

The general time reversible model with gamma distribution and invariant sites (GTR+Γ_5+ I) was selected as the best fitting substitution model based on the jModelTest (Darriba et al., 2012) analysis. In order not to assume any particular demographic scenario as a priori, a relaxed uncorrelated lognormal clock (Drummond et al., 2006) and the Bayesian skyline plot (BSP) coalescent model (Lemey et al., 2009) was used to estimate the most probable origin, nucleotide substitution rate and the time to most recent common ancestor (tMRCA) of different lineages. Because the empirical evidence suggests that DENV-1 lineages evolve at different rates (Goncalvez et al., 2002), a strict clock was not preferred. The prior for the substitution rate was set at default settings to allow estimation of the rates among tree branches (Pls see supplemental Data File S1 for prior information). The MCMC chain was run for 200 million generations

sampling every 20,000 states. The effective sampling size (ESS) values of more than 200 were considered as a sufficient level of sampling. The posterior tree distribution was summarized using TreeAnnotator v.1.7.4 program (Drummond and Rambaut, 2007), with 10% burn-in and the final MCC tree was visualized using FigTree v.1.4.3 (http://tree.bio.ed.ac.uk/software/figtree/).

Assigning of locations to each sequence

In Singapore, dengue control is a joint effort between the National Environment Agency (NEA) and the Ministry of Health (MOH). The effort is backed up by a strong surveillance framework that includes cases, virus and vectors. Cases are reported through a mandatory notification system. All cases are laboratory confirmed. Once a case is confirmed, MOH conducts an epidemiological investigation that includes interviewing patients whenever possible to determine whether a case is imported or locally acquired. If locally acquired, MOH provides the postal code information of the most probable location of infection for each case. This could be the residential, workplace or any other address. In the present study, we used location data assigned by MOH to each case. The arbovirus surveillance programme uses this data to monitor the spatial distribution of virus strains on a weekly basis, with a view of mapping those that establish autochthonous transmission. NEA uses this information to define dengue disease clusters and thereby to identify hotspots of DENV transmission.

Phylogeography analysis of envelope gene sequences

Partitioning Around Mediods (PAM) was used to geocluster virus data into distinct clusters based on postal code information assigned to each sequence. PAM is a partitioning technique of clustering that minimizes the distance between a particular point in a cluster and the point designated as the centre of the cluster. The average distance to the next nearest postal code (18 m for the analysed dataset) was calculated by using the "calculate distance band from neighbour count" tool in ArcGIS 10.5. Using the geographical distance of cases as the dissimilarity measure, the respective virus sequences were grouped into 10 clusters. The average distance between two clusters was 5,250 m (Range: 2,986-6,027 m). The optimal number of clusters (k=10) was determined by comparing the Silhouette width of different cluster numbers.

The complete *E* gene sequences of 792 randomly selected DENV-1 strains from 10 defined geographical locations were used for phylogeography analysis. At least one representative was chosen from a group of identical sequences from each location per epidemiological week (EW). jModelTest (Darriba et al., 2012) suggested the Tamura-Nei model with gamma rate categories ($TN93+\Gamma_5$) as the best-fitting substitution model. The analyses were performed using a flexible Bayesian skyline demographic prior and a relaxed uncorrelated lognormal clock (Drummond et al., 2006). A Bayesian Stochastic Search Variable Selection (BSSVS) procedure was used to identify significant diffusion pathways among 10 clusters included in the discrete phylogeographic analysis (Lemey et al., 2009) (Pls see supplemental Data File S2 for prior information). Four MCMC analyses for 100 million generations each, sampling every 10,000 states, were combined in LogCombiner (http://tree.bio.ed.ac.uk/software), after removing 10% burn-in. SPREAD 1.0.4 (Bielejec et al., 2011) was used to analyse phylogeographic reconstructions resulting from Bayesian inference of spatiotemporal diffusion of tests established. Bayes factor (BF) values were calculated by comparing the posterior and prior probability of the individual rates in order to test the significant linkage between locations. A

BF>3 was considered well-supported, with classifications of substantial (BF>3), strong (BF>10), very strong (BF>30) and decisive (BF>100) (Faria et al., 2013; Lemey et al., 2009). The diffusion links between locations were visualized in Google Earth.

Selection pressure analysis

The selection pressure acting on each codon of whole genomes was measured by the ratio of non-synonymous to synonymous rates (dN/dS) computed in HyPhy open-source software package as implemented in Datamonkey web-server (Delport et al., 2010). Single likelihood ancestor counting (SLAC), fixed effects likelihood (FEL), internal fixed effects likelihood (IFEL), mixed effect model of evolution (MEME) and fast unbiased Bayesian approximation (FUBAR) methods were used to estimate the sites under selection. The GTR nucleotide substitution bias model (REV) and neighbour joining phylogeny were used as analytical parameters in different approaches. An integrative approach recommended previously (Delport et al., 2010) was employed in ascertaining the positive or negative selection at each site. The sites which were found to be non-neutral and be positively or negatively selected by all methods, and by at least three methods at significant levels were considered to be positively/negatively selected sites. The p-values = < 0.05 were considered as significant for SLAC, FEL, IFEL and MEME methods, whereas the posterior probability value of = > 0.9 was used for FUBAR.

Secondary structure analysis of 3'untranslated region

The secondary structures of DENV-1 3' untranslated region (UTR) of different lineages were predicted using the mfold web server (Zuker, 2003) at http://mfold.rna.albany.edu/?q=mfold under standard conditions (37^0C). The analysis included the complete sequences of 3' UTR.

***In vitro* replication kinetics**

Virus stock preparation

We determined the replication kinetics of 10 DENV-1 strains of genotypes I and III. They included six strains that established sustained transmission during the study period (Genotype III 2011; SG(EHI)D1/15834Y11; NCBI accession no. JN544407, Genotype III 2012; SG(EHI)D1/18640Y12; NCBI accession no. MG097875, Genotype III 2013; SG(EHI)D1/44259Y12; NCBI accession no. KM403575, Genotype Ia; SG(EHI)D1/04009Y13; NCBI accession no. KJ806953, Genotype Ib; SG(EHI)D1/30889Y14; NCBI accession no. MG097876, Genotype Ic; SG(EHI)D1/09063Y15; NCBI accession no. MF033232), two genotype III isolates reported in isolated cases in 2009 (SG(EHI)D1/0091Y09; NCBI accession no. JF960211) and 2011 (SG(EHI)D1/09106Y11; NCBI accession no. JN544409) as well as two genotype I isolates reported during the epidemic in 2005 (D1/SG/05K4441DK1/2005; NCBI accession no. EU081266 and D1/SG/05K4443DK1/2005; NCBI accession no. EU081267). All isolates were scaled-up up to four passages by using 25 µl of stock solution in *Aedes albopictus* C6/36 cell line (ATCC CRL 1660) as described in the virus isolation for genome sequencing section, to obtain a virus titre of at least 10^5 plaque-forming units (PFU) per ml. Virus stocks were kept at -80°C until further use.

Replication kinetics assay

Hepatoma cell line Huh-7 (Courtesy of Prof. Justin Chu, National University of Singapore) and *Aedes albopictus* C6/36 cell line (ATCC CRL 1660) were used to determine the replication kinetics of DENV-1 lineages in mammalian and mosquito cells respectively. These two cell lines have commonly been used by previous similar studies (Manokaran et al., 2015; Tajima et al., 2006). Huh-7 cells were scaled-up in Dulbecco's modified Eagle's medium (DMEM, Biopolis Shared Facilities, A*Star, Biopolis, Singapore) at 37°C with 5% CO2. The media contained 10% heat-inactivated Foetal Bovine Serum (FBS), 1% L-glutamine solution, 100 mM Penicillin/Streptomycin, 7.5% sodium bicarbonate and 10 mM HEPES. *Aedes albopictus* cell line (C6/36, ATCC CRL 1660) was scaled-up at 28°C in Leibowitch L-15 medium (Invitrogen Corp., Carlsbad, CA, USA), supplemented with 10% FBS, 1% L-glutamine solution and 100 mM Penicillin/Streptomycin. Maintenance medium for each cell line was similarly prepared, but supplemented with 3% FBS.

Huh-7 and C6/36 cells were seeded at ~2 x 10^5 cells in 24 well plates to approximately 85-90% confluence, before infecting with DENV-1 strains at multiplicity of infection (MOI) of 0.1 in duplicates. After one-hour adsorption at 37˚C, each virus suspension was removed and cells were washed twice with phosphate buffered saline (PBS). The cells were then incubated in maintenance media at 37°C for up to five days. Supernatants were harvested at 0 hr and every 24 hrs subsequently up to 120 hrs (0 to 5 days) post infection (hpi) and infectious viral titres were determined by plaque assay.

Quantification of infectious virus particles by plaque assay

Baby Hamster Kidney cells (BHK-21, courtesy of Novartis Institute of Tropical Diseases) were used to perform the plaque assay (Manokaran et al., 2015; Tan et al., 2013). BHK-21 cells were scaled-up in RPMI medium (Sigma-Aldrich Corp., St. Louis, MO, USA) at 37°C with 5% CO2. The plaque assay for the quantification of infectious virus titres was carried out for each virus as described elsewhere (Tan et al., 2013). In brief, BHK-21 cells were seeded in 24 well plates to obtain a monolayer of cells at 90-95% confluence. The viruses were serially diluted from 1:10^{-1} to 1:10^{-6} using serum-free culture media. Following one-hour adsorption, virus inoculum was discarded and 1.5% complete carboxymethyl cellulose (CMC) medium was added. At day 5, BHK-21 cells were fixed with 20 % formalin and stained with naphthol blue stain solution. Plaques were counted and expressed as PFU/ml.

Amplification of genomic and sub-genomic RNA

DENV-1 total RNA was extracted from infected cells using the QIAGEN QIAamp viral RNA mini kit (QIAGEN, Hilden, Germany) according to manufacturer's recommendations. DENV-1 genomic (gRNA) and sub-genomic (sfRNA) RNA levels were measured by using a SYBR green I-based one-step real-time quantitative RT-PCR assay carried out on a LightCycler® 2.0 (Roche Diagnostics GMbH, Mannheim, Germany). Primer gD1-F (5' AGCCATAGCACGGTAAGAGC 3') targeted the upstream (coding) region of DENV-1 3'UTR and captured gRNA and sfRNA. On the other hand, primer sfD1+3 (5' CCGTCCAAGGACGTAAAATG 3') was designed within the DENV-1 sfRNA region to capture any excess sfRNA production. We used a single reverse primer sfD1+3-R (5' CCCTCCCAAGACACAACGCAGC 3') that generated 211 bp (gRNA+sfRNA) and 174 bp (sfRNA) amplicons. The RT-PCR was performed by using QuantiTect SYBR Green RT-PCR Kit (Qiagen, Hilden, Germany) with 1 µl of RNA template and 1 µM of each primer in 10 µl reactions. The thermal profile of RT-PCR was 60°C for 10 min

and 95°C for 0 s, followed by 35 cycles of 94°C for 0 s, 46-50°C for 3 s and 72°C for 10 s, melting at 70°C for 30 s and a cooling step of 40°C for 30 s.

Quantification of genomic and sub-genomic RNA copy numbers

The concentration of purified amplicons of gRNA and sfRNA was measured in a NanoDrop spectrophotometer (NanoDrop Technologies, Inc. DE) and were cloned into the vector at an insert: vector ratio of 3:1 by using the NEB PCR cloning kit (New England Biolabs, USA) according to manufacturer's instructions. The presence of cloned inserts was confirmed by colony PCR. The plasmid minipreps were prepared by using the Wizard plus SV minipreps DNA purification kit (Promega Corporation, Madison, WI). The inserts were obtained after digestion with EcoRI (New England Biolabs, USA) and were gel purified by using the QIAquick Gel Purification kit (Qiagen, Hilden, Germany). The insert yield was quantified as above and copy numbers were calculated based on the product size and DNA concentration. The purified inserts were 10-fold serially diluted from 10^8 to 10^{-4} copies/ul and RT-PCR was performed for each dilution as described above. The standard curve, obtained by plotting quantification cycle values against known copy numbers for each dilution, was used to quantify the number of RNA copies in study samples. The ratio of sfRNA: gRNA copies was calculated to determine if any of the virus strains produced excess sfRNA.

Supplemental References

Bielejec, F., Rambaut, A., Suchard, M.A., and Lemey, P. (2011). SPREAD: spatial phylogenetic reconstruction of evolutionary dynamics. Bioinformatics *27*, 2910-2912.

Darriba, D., Taboada, G.L., Doallo, R., and Posada, D. (2012). jModelTest 2: more models, new heuristics and parallel computing. Nat Methods *9*, 772.

Delport, W., Poon, A.F., Frost, S.D., and Kosakovsky Pond, S.L. (2010). Datamonkey 2010: a suite of phylogenetic analysis tools for evolutionary biology. Bioinformatics *26*, 2455-2457.

Drummond, A.J., Ho, S.Y., Phillips, M.J., and Rambaut, A. (2006). Relaxed phylogenetics and dating with confidence. PLoS Biol *4*, e88.

Drummond, A.J., and Rambaut, A. (2007). BEAST: Bayesian evolutionary analysis by sampling trees. BMC Evol Biol *7*, 214.

Faria, N.R., Suchard, M.A., Rambaut, A., Streicker, D.G., and Lemey, P. (2013). Simultaneously reconstructing viral cross-species transmission history and identifying the underlying constraints. Philos Trans R Soc Lond B Biol Sci *368*, 20120196.

Gan, V.C., Tan, L.K., Lye, D.C., Pok, K.Y., Mok, S.Q., Chua, R.C., Leo, Y.S., and Ng, L.C. (2014). Diagnosing Dengue at the Point-of-Care: Utility of a Rapid Combined Diagnostic Kit in Singapore. PLoS One *9*, e90037.

Goncalvez, A.P., Escalante, A.A., Pujol, F.H., Ludert, J.E., Tovar, D., Salas, R.A., and Liprandi, F. (2002). Diversity and evolution of the envelope gene of dengue virus type 1. Virology *303*, 110-119.

Hall, T.A. (1999). BioEdit: a user-friendly biological sequence alignment editor and analysis program for Windows 95/98/NT. Nucl Acid Symp Ser *41*, 95-98.

Hapuarachchi, H.C., Koo, C., Kek, R., Xu, H., Lai, Y.L., Liu, L., Kok, S.Y., Shi, Y., Chuen, R.L., Lee, K.S*., et al.* (2016). Intra-epidemic evolutionary dynamics of a Dengue virus type 1 population reveal mutant spectra that correlate with disease transmission. Sci Rep *6*, 22592.

Koo, C., Nasir, A., Hapuarachchi, H.C., Lee, K.S., Hasan, Z., Ng, L.C., and Khan, E. (2013). Evolution and heterogeneity of multiple serotypes of Dengue virus in Pakistan, 2006-2011. Virol J *10*, 275.

Lai, Y.L., Chung, Y.K., Tan, H.C., Yap, H.F., Yap, G., Ooi, E.E., and Ng, L.C. (2007). Cost-effective real-time reverse transcriptase PCR (RT-PCR) to screen for Dengue virus followed by rapid single-tube multiplex RT-PCR for serotyping of the virus. J Clin Microbiol *45*, 935-941.
Lemey, P., Rambaut, A., Drummond, A.J., and Suchard, M.A. (2009). Bayesian phylogeography finds its roots. PLoS Comput Biol *5*, e1000520.
Manokaran, G., Finol, E., Wang, C., Gunaratne, J., Bahl, J., Ong, E.Z., Tan, H.C., Sessions, O.M., Ward, A.M., Gubler, D.J*., et al.* (2015). Dengue subgenomic RNA binds TRIM25 to inhibit interferon expression for epidemiological fitness. Science *350*, 217-221.
Tajima, S., Nukui, Y., Ito, M., Takasaki, T., and Kurane, I. (2006). Nineteen nucleotides in the variable region of 3' non-translated region are dispensable for the replication of dengue type 1 virus in vitro. Virus research *116*, 38-44.
Tan, L.K., Lam, S., Low, S.L., Tan, F.H., Ng, L.C., and Teo, D. (2013). Evaluation of Pathogen Reduction Systems to Inactivate Dengue and Chikungunya Viruses in Apheresis Platelets Suspended in Plasma. Advances in Infectious Diseases *Vol.03No.01*, 9.
Zuker, M. (2003). Mfold web server for nucleic acid folding and hybridization prediction. Nucleic Acids Res *31*, 3406-3415.